1 **MUDA: dynamic geophysical and geochemical MUltiparametric DAtabase**

Marco Massa [1], Andrea Luca Rizzo [1,2], Davide Scafidi [3], Elisa Ferrari [1], Sara Lovati [1], Lucia Luzi [1] and MUDA WG (*)

2

3 [1] National Institute of Geophysics and Volcanology (INGV), Milano department, Italy

[2] University of Milano Bicocca, DISAT, Milano, Italy

[3] University of Genova, DISTAV, Genova, Italy

4

5 (*) A full list of authors appears at the end of the paper

6

7 Corresponding author: marco.massa@ingv.it

8

9 **Abstract**

10   In this paper, the new dynamic geophysical and geochemical MUltiparametric DAtabase

11 (MUDA) is presented. MUDA is a new infrastructure of the National Institute of Geophysics and

12 Volcanology (INGV), published on-line in December 2023, with the aim of archiving and

13 disseminating multiparametric data collected by multidisciplinary monitoring networks. MUDA is a

14 *MySQL* relational database with a web interface developed in *php,* aimed at investigating in quasi real

15 time possible correlations between seismic phenomena and variations in endogenous and

16 environmental parameters. At present, MUDA collects data from different types of sensors such as

17 hydrogeochemical probes for physical-chemical parameters in waters, meteorological stations,

18 detectors of air Radon concentration, diffusive flux of carbon dioxide (CO_2) and seismometers

19 belonging both to the National Seismic Network of INGV and to temporary networks installed in the

20 framework of multidisciplinary research projects. MUDA daily publishes data updated to the previous

21 day and offers the chance to view and download multiparametric time series selected for different

22 time periods. The resultant dataset provides broad perspectives in the framework of future high

23 frequency and continuous multiparametric monitoring as a starting point to identify possible seismic

precursors for short-term earthquake forecasting. MUDA is now quoted with the Digital Object Identifier https://doi.org/10.13127/muda (Massa et al., 2023).

1 Introduction

Today, there is an increasing awareness of the role played by the interaction between tectonics and fluid dynamics in triggering seismicity. Yet, the simultaneous monitoring of the relevant key factors is still lacking, even though it could be crucial in recognizing precursory signals. Changes in water chemistry and levels, spring discharges, soil flux regimes (e.g. CO_2, CH_4, Radon) and compositions of dissolved gases in water are well-documented in the literature (e.g. Italiano et al., 2001, 2004; Chiodini et al., 2020; Gori and Barberio, 2022 and references therein), as being pre-, co- and post-seismic modifications as well as markers of the local tectonic stress acting in the crust. These recognized seismic-induced variations in groundwaters and springs led, in recent years, scientists to give more attention to the development of multiparametric monitoring, in order to capture the main evidences concerning abrupt changes in chemical and physical parameters recorded before (and also after) energetic seismic events (Rikitake and Hamada, 2003; Cicerone et al., 2009; Martinelli, 2018 and references therein). The ultimate goal is to find systematic signals that can be assumed as possible "precursors" or indicators that a seismogenetic process is ongoing (Hubbert and Rubey, 1959; Brauer et al., 2003; Miller et al., 2004; Chiarabba et al., 2009; Di Luccio et al., 2010; Malagnini et al., 2012; Keranen and Weingarten, 2018; Napolitano et al., 2020; De Matteis et al., 2021; Gabrielli et al., 2022, 2023; Ventura and Di Giovambattista, 2013). At the Italian scale, several studies have described the utility of groundwater and spring parameters and soil gas emissions to catch seismic-related signals as well. However, only a few studies reported a continuous, high-frequency monitoring, mainly of groundwater level or hydraulic pressure (De Gregorio et al., 2012; Barberio et al., 2017; De Luca et

al., 2018), or as Gori and Barberio (2022) concerning spring monitoring (i.e. temperature, pH, electrical conductivity, dissolved oxygen and carbon dioxide) or D'Alessandro et al. (2020) on soil Radon emissions related to seismic activity.

MUDA (geophysical and geochemical MUltiparametric DAtabase), a new dynamic multiparametric database published on-line in December 2023 at the web site https://muda.mi.ingv.it (Figure 1), has been developed in such a framework. MUDA is a new infrastructure of the National Institute of Geophysics and Volcanology (INGV, www.ingv.it) devoted to archive daily and distribute quasi real time geophysical and geochemical multiparametric data recorded in continuous or near-continuous mode at selected sites installed at the most tectonically active Italian areas (Figure 2). MUDA was designed in the framework of INGV Dynamic Planet S2-project (i.e. 3D structure of Italy from multidata analysis. Passive/active seismic, magnetic, magnetotelluric, electrical, gravimetric prospecting, https://progetti.ingv.it/it/pian-din) and its development is ongoing in the framework of the INGV Dynamic Planet GEMME project (Integrated Geological, gEophysical and geocheMical approaches for 3D Modelling of complex seismic site Effects).

The need for an infrastructure capable of acquiring, storing, organising and publishing multiparameter data in near real time arose following the installation of the Garda multiparameter seismic network, PDnet (https://eida.ingv.it/it/networks/network/ZO), installed starting from 2021 as part of the Task-S2 of the INGV Dynamic Planet project (Massa et al., 2021; Ferrari et al., 2024). In this framework, MUDA collects information from different types of sensors, such as seismometers, accelerometers, hydrogeochemical for physical-chemical parameters in waters, geochemical for measuring the diffusive flux of carbon dioxide (CO_2) from the soil or detecting the air Radon concentration, and meteorological stations. The aim is to constraint the influence due to exogenous parameters in order to make potential correlations between seismic phenomena and variations concerning monitored parameters (i.e. groundwater level, temperature, electrical conductivity, CO_2 soil flux, air Radon concentration; Barberio et al., 2017; Chiodini et al., 2020; Mastrorillo et al., 2020).

76 The challenge of MUDA is to provide the end-user a high quality dynamic but also

77 simultaneous and continuous monitoring of groundwater physical parameters, meteorological data

78 and seismic signals, together with gas concentration such as Radon or soil CO_2-CH_4 fluxes (Figure

79 3). In order to furnish the main information for a detailed interpretation of local phenomena in the

80 framework of multi-hazard assessment, the multiparametric data are provided together with all

81 necessary stations and sites metadata, supplied with a complete geological and morphological

82 description (Figure 4).

83

84 **2 Seismotectonic framework and seismicity**

85

86 The multiparametric sites now included in MUDA are located in five main target areas (Figure

87 2): Lake Garda, eastern Alps, Po alluvial basin, Northern and Central Apennine chains (Table 1).

88 Concerning instrumental seismicity (http://terremoti.ingv.it/), in the last 40 years, thousands of small

89 to moderate energy seismic events (Figure 2) occurred in Northern Italy. Despite the low-to-medium

90 seismic hazard of the area (Stucchi et al., 2011), the high level of exposure (e.g. metropolitan areas,

91 industrial plants etc.), the local geological condition and the proximity of active buried seismogenic

92 structure (Burrato et al., 2012) make many portions of North Italy a medium to high seismic risk zone

93 (Massa et al., 2022b, Lai et al., 2020).

94 In particular, the Garda region (Area 1, Figure 2) is characterized by low-to-moderate

95 seismicity with the active tectonic regime located on the margin of the southern Alpine chain

96 controlled by the Africa-Europe convergence. The main active faults affecting the area consist of

97 mainly NNE-SSW trending thrusts (Galadini et al., 2001). For instance, the November 24, 2004,

98 Vobarno M_w 4.8 earthquake (https://terremoti.ingv.it/event/1564989), generated maximum

99 macroseismic intensities (Imax) of VII/VIII (https://emidius.mi.ingv.it/CPTI15-DBMI15/, Locati et

100 al., 2022). It is worth noting that in the past the same area was struck by several powerful events, such

4

as the October 30, 1901, Salò M_w=5.4 earthquake (https://emidius.mi.ingv.it/CPTI15-DBMI15/, Rovida et al., 2022).

Moving eastwards (Area 2, Figure 2), the highest rate of energetic events in Northern Italy is associated to the South-verging thrust faults typical of the central and East South Alpine Chain (Battaglia et al., 2004; Serpelloni et al., 2005; D'Agostino et al., 2008), due to the North-South convergence between the Adriatic microplate and the Alps. The most recent destructive earthquake occurred in Friuli, during the seismic sequence of May 6, 1976, with M_w= 6.5 (Pondrelli et al., 1999 and reference therein), whereas the largest historical event was the 1695 Asolo earthquake, with an estimated M_w=6.48 (https://emidius.mi.ingv.it/CPTI15-DBMI15/) broadly associated to the thrust system of the Montello area (Danesi et al., 2015).

South of the Alps, the Po alluvial plain (Area 3, Figure 2) represents a very deep foreland basin of two opposing verging fold-and-thrust belts developing in the framework of the African and European plates relative convergence (Pieri and Groppi, 1981; Bigi et al., 1990). Despite the flat morphology, the Po plain is far from being an undeformed domain, since the outermost and most recent thrust fronts of the two belts are buried by the Plio-Quaternary sedimentary sequence (Burrato et al., 2012). The historical and instrumental Italian seismic catalogues show that the southern Po plain is affected by low to moderate seismicity, with M_w up to 5.8 during the 2012 sequence (Luzi et al., 2013). Considering the historical seismicity (Rovida et al., 2020), the central part of the Po plain was struck by the more significant North Italy earthquake on January 3, 1117, with an estimated M_w=6.52.

Moving southwards, the Northern Apennines (Area 4, Figure 2) underwent the regional seismicity associated with the Apennine fronts defined by different arcs of blind, North-verging thrusts and folds (Mazzoli et al., 2015; Chiaraluce et al., 2017), capable of generating moderate energetic seismic events with a maximum magnitude around 6 (i.e. June 5, 1501, M_w 6.05, Rovida et al., 2022). In particular, this area hosts the Nirano site (Table 1), in the Regional Natural Reserve of Salse di Nirano (Giambastiani et al., 2024; Romano et al., 2023), an area lying upon an anticline

127 structure of the North-East verging fold-and-thrust Apennine belt characterized by one of the largest

128 mud volcano fields in Europe (Bonini, 2008; Castaldini et al., 2005) coupled to the emission of CH_4-

129 dominated gases (e.g., Buttitta et al., 2020).

130 Finally, two stations included in MUDA, are installed in the surroundings of the Norcia

131 alluvial basin (Area 5, Figure 2), an area characterized by high seismic hazard and seismicity rate due

132 to dense extensional NW-SE active fault systems (e.g. Galadini et al., 1999, Brozzetti and Lavecchia,

133 1994) capable of generating high-magnitude earthquakes (Galli et al., 2018; 2019), such as the

134 January 14, 1703, M_w=6.9, earthquake or other moderate events such as the 1328, M_w=6.3, the 1730,

135 M_w=5.9, the 1859, M_w=5.5 and the 1979, M_w=5.8, earthquakes (Rovida et al, 2022). The recent

136 instrumental seismicity highlights the two main events occurring on August 24, 2016 and on the

137 October 30, 2016, with M_w 6.0 and 6.5 respectively, in an area a few kilometres of the Norcia plain

138 (e.g. Improta et al., 2019 and reference therein).

139

140 **3 State of the art**

141

142 At present, in Italy and Europe, the seismological communities in general are fairly advanced

143 in their running of both network data management and seismic data sharing. In Italy, the main seismic

144 network is represented by the National Seismic Network (RSN,

145 https://eida.ingv.it/it/networks/network/IV, Margheriti et al., 2020), managed by INGV and

146 sometimes integrated for real time data exchange by many local or regional networks (Massa et al.,

147 2022). The RSN permanent network is codified through the IV code assigned by the International

148 Federation of Digital Seismograph Networks, FDSN (https://www.fdsn.org/). The RSN station codes

149 are registered at International Seismological Center, ISC (http://www.isc.ac.uk/), while data, recorded

150 following the SEED (Standard for the Exchange of Earthquake Data,

151 http://www.fdsn.org/seed_manual/SEEDManual_V2.4.pdf) format, are shared (Danacek et al., 2022)

152 through the EIDA-Italia node (European Integrated Data Archive, https://eida.ingv.it/it/). In Italy,

153 INGV provides many websites and thematic databases for real time data quality and distribution,

154 such as EIDA-Italia, ISMDq (INGV Strong Motion Data quality, https://ismd.mi.ingv.it , Massa et

155 al., 2022), ITACA (ITalian Accelerometric Archive, https://itaca.mi.ingv.it, Pacor et al., 2011), ESM

156 (Engineering Strong Motion database, https://esm-db.eu/, Luzi et al., 2016), BSI (Italian Seismic

157 Bulletin, https://terremoti.ingv.it/bsi, Marchetti et al., 2016), TDMT (Time Domain Moment Tensor,

158 https://terremoti.ingv.it/tdmt, Scognamiglio et al., 2009), ShakeMaps (https://shakemap.ingv.it/,

159 Michelini et al., 2020), etc.

160 Differently, the geochemical community has still not developed a so capillary network of automatic

161 stations for data acquisition, management and sharing, as the seismic community does. This mostly

162 depends on the fact that only a few geochemical parameters/tracers can be measured directly in the

163 field and in near real-time [e.g., diffusive flux of CO_2 from the soil through accumulation chamber

164 method (Chiodini et al., 1998; Carapezza et al., 2004; Inguaggiato et al., 2011a; Rizzo et al., 2015),

165 Radon concentration in atmosphere or from the soil with specific Geiger counters, concentration of

166 H_2O, CO_2, SO_2, H_2S, CH_4, halogens in atmosphere through MULTIGAS sensors (Aiuppa et al., 2005;

167 Shinohara et al., 2005) or FTIR technique (e.g., Allard et al., 2005), SO_2 flux in atmosphere by DOAS

168 and UV techniques (Burton et al., 2009; Aiuppa et al., 2021)]. It must be also highlighted that most

169 of the automatic measurements of geochemical parameters above reported were developed and

170 applied in volcano monitoring, while only recently the geochemical community is moving to apply

171 some of those tracers to seismic monitoring. In terms of hydrogeochemical monitoring, apart the

172 physical-chemical parameters in water (e.g., temperature, water level, electric conductivity, and

173 others such as pH and Eh but with less precision and accuracy) for which automatic sensors exist

174 since long time, the automatic and high-frequency measurement of the water's composition is limited

175 to a few sensors developed in the last decade or so, which mostly focus on the concentration of a few

176 gas species dissolved in waters (e.g., CO_2, CH_4, total gas pressure; De Gregorio et al., 2005,

177 Inguaggiato et al., 2011b). As for gas sensors, most of the automatic measurements of water's

178 composition were developed for volcano monitoring applications.

179   At present, in Italy, hydrogeochemical and geochemical seismic monitoring is limited to

180   selected areas or sites, and it is essentially performed by several departments of INGV in the

181   framework of individual initiative such as the Alto Tiberina Near Fault Observatory (TABOO,

182   https://ingv.it/en/monitoring-and-infrastructure-a/monitoring-networks/the-ingv-and-its-

183   networks/taboo, Chiaraluce et al., 2014) or recent and on-going INGV projects such as the Dynamic

184   Planet (https://progetti.ingv.it/it/pian-din), FURTHER (https://progetti.ingv.it/en/further), MYBURP

185   (https://progetti.ingv.it/it/pian-din#myburp-modulation-of-hydrology-on-stress-buildup-on-the-

186   irpinia-fault), Multiparametric Networks or Rebuilding Central Italy, DL50 and related tasks (e.g.

187   Idro-DEEP CO_2, Idro-Calabria, Idro-Nord), concerning the groundwater continuous monitoring (e.g.

188   springs and thermal waters) of different areas of mainly Central and Southern Italian Apennines

189   (https://www.pa.ingv.it/index.php/progetti/)   and   Radon   monitoring   (IRON   project,

190   https://ingv.it/monitoraggio-e-infrastrutture/reti-di-monitoraggio/l-ingv-e-le-sue-reti/iron).   In

191   particular, the Alto Tiberina Near Fault Observatory is managed by EPOS (European Plate Observing

192   System) research infrastructure (https://www.epos-eu.org/) of which the mission is to foster the

193   integration of solid earth data and their by-products made by the entire European scientific

194   community: in this case, seismological, geophysical, geodetic and geochemical data recorded by

195   TABOO-Near Fault Observatory are accessible via the FRIDGE European web portal

196   (https://fridge.ingv.it/index.php).

197   Further local monitoring initiatives are provided by other institutions or Universities through

198   the installation of geochemical stations and probes in different parts of the national territory such as

199   in Tus**ca**ny, by the IGG-CNR (Institute of Geoscience and Earth Resources,

200   https://www.igg.cnr.it/en), in Southern Italy, by the IMAA CNR (Institute of methodologies for

201   environmental analysis, https://www.cnr.it/en/institute/055/institute-of-methodologies-for-

202   environmental-analysis-imaa) or Central Italy, by the Earth Sciences Department (DES,

203   https://www.dst.uniroma1.it/en) of Sapienza University of Rome (Martinelli et al., 2021).

204   Consequently, at a national scale the hydrogeochemical and geochemical monitoring is not

205   organized by using an ad hoc reference institutional database or web portal able to homogeneously

206   archive and distribute high quality multiparametric data to the scientific community. At present and

207   at the best of our knowledge, the only existent databases focus only on mapping gas emissions (e.g.,

208   MaGa, http://www.magadb.net/) or thermal springs, without archiving data from a regular

209   monitoring. A first attempt was recently made in the framework of an agreement between the National

210   Institute of Geophysics and Volcanology (INGV) and the National System for Environmental

211   Protection (SNPA, https://www.snpambiente.it/, comprising the Regional Environmental Protection

212   Agencies, ARPA, and the Italian Institute for Environmental Protection and Research, ISPRA,

213   https://www.isprambiente.gov.it/), with the aim of sharing data from the continuous monitoring of

214   water wells and springs, in particular the piezometric level, temperature, electrical conductivity,

215   salinity and total dissolved solids (Comerci et al., 2019).

216

217   **4 MUDA database**

218

219   MUDA is a dynamic and relational multiparametric database designed and built using a table

220   structure that can correlate data of a different nature (i.e. seismic, hydrogeochemical, geochemical,

221   meteorological). It is adaptable to further types of data from other projects and capable of integrating

222   perfectly with those already acquired via both real time and off-line transmission vectors (Figure 5).

223   The MUDA database is based on MySQL (https://www.mysql.com/it/), a popular and efficient open-

224   source relational database management system for handling large amounts of data. Particular attention

225   has been paid to optimising and, above all, integrating all the different types of data taken from

226   different sources while trying to maintain a certain structural uniformity, also open to possible future

227   new implementation.

228   Data collection takes place separately for each type of monitoring station (Table 1), each according

229   to its preferred channels (email, ftp system, Application Programming Interface API, Structured

Query Language SQL) with the effort to improve each procedure, avoid data loss and minimise the time taken to receive data.

Data are acquired and then archived on a centralised server from which all pre-processing procedures are then carried out to insert this data, after appropriate checks and automatic analysis, into the MUDA database (see next chapter for details). All data downloaded from the remote stations, after the check and processing phase are stored in files before the population of the MySQL database. This is also convenient to have a native and complete data backup, for future requirements.

The MUDA database is structured to consider all the different types of monitoring stations at the same multiparametric site through a univocal internal site code, linked to all different types of data. At the same time, however, the independence of the data of each different station is also maintained, as each individual site may have its own particular condition and metadata. For each type of monitoring station, the MUDA database includes 2 tables, one for the station metadata and the other for the recorded data, linked by a unique station id.

4.1 Processing of raw data

The MUDA project currently includes 5 types of data: hydrogeochemical, meteorological, Radon, CO_2 and seismic. All data are pre-processed to align each time series to the common UTC (Coordinated Universal Time) time. Hydrogeochemical, seismic, meteorological and Radon data are moreover resampled in order to have a representative data each few minutes (i.e. from 1 to 5), namely a good enough interval to see possible cross-correlation signals on different parameters. A data resample is a priori necessary in order to, at first, homogenize data for viewing and comparison, but also to allow the web page to have a fast response to any query involving long time periods (actually up to a maximum of 30 days) of continuous and high frequency multiparametric recordings. In particular, while hydrogeochemical, gas and meteorological data are uploaded into MUDA database as raw data with only a consistency check, the seismic data are pre-processed in order to obtain

256 waveforms metadata to be included into MUDA database and to be easily comparable in terms of

257 time series to the other parameters.

258 The processing of raw data for each of the 5 parameters included in MUDA is described in detail in

259 the following.

260

261 The hydrogeochemical data are acquired by two different types of instrumentation, the first

262 provided by Van Essen Instruments (https://www.vanessen.com/) and the second by STS-Italia S.r.l.

263 (https://www.sts-italia.it/). Data recorded by Van Essen Instruments and STS-Italia are set to sample

264 records everyone and ten minutes, respectively. In both cases, groundwater level (m), electrical

265 conductivity (µS/cm), and temperature (C°) are achieved using probes (e.g. CTD-Diver®,

266 https://www.vanessen.com/) installed in correspondence of wells or springs by using weir

267 flowmeters; the recorded chemical and physical parameters are sent at defined time intervals to the

268 remote company head offices and then to the INGV acquisition centre by proprietary API or email.

269 At present, remote stations send data in ASCII format twice a day (i.e. 9 a.m. and 9 p.m., Central

270 European Time, CET) as an email attachment or by ftp-protocol. Depending on the target

271 instrumentation, before populating the MUDA database, a pre-processing is necessary: as an example,

272 the Van Essen probes for water wells need a barometric compensation to account for atmospheric

273 pressure variations in order to provide the corrected water level value (Ferrari et al., 2024). Automatic

274 data acquiring and processing tools have been developed in Python (https://www.python.org/), while

275 automatic tools for populating the MUDA database have been developed in PHP language

276 (https://www.php.net).

277

278 The meteorological data included in MUDA are provided by Davis Vantage Vue®

279 instrumentation (https://www.davisinstruments.com/). Each single meteorological station, placed

280 near the water well, provides information on atmospheric pressure (mbar), temperature (C°), humidity

281 (%), rainfall amount (mm), wind speed and direction. Also in this case, data take advantage of

GPRS/LTE technologies and are gathered by a dedicated WeatherLink Live cloud platform, making them available in real time on the dedicated website (https://www.weatherlink.com/). With samples every one minute, data are archived into the Davis server-cloud and then shared by payment to the end-users (e.g. INGV server) through proprietary Application Programming Interface (API) set into an automated ad-hoc developed python tool, suited for all the different kinds of meteorological instrumentation at each site. Just as for hydrogeochemical data, meteorological parameters are then automatically inserted into the MUDA database twice a day (i.e. 9 a.m. and 9 p.m. CET) using a procedure developed in PHP.

The Radon data are provided by the IRON network (Italian Radon mOnitoring Network, https://ingv.it/monitoraggio-e-infrastrutture/reti-di-monitoraggio/l-ingv-e-le-sue-reti/iron, Cannelli et al., 2018). Stations, placed next to the water well, measure the concentration of gas in the air using a photodiode detector (AER Plus, Algade), with a sensitivity of 15 Bq/m^3 by counts/hour. Data are measured and acquired every 4 hours together with temperature and humidity, Radon data are transmitted in real time by the Sigfox (https://www.sigfox.com) 0G-technology and archived at the Sigfox cloud, with the exception of particularly remote sites where a periodic local data downloading is also necessary. Radon data are provided in csv format, where the concentration is measured in Bq/m^3, and then uploaded into the MUDA database using an ad-hoc developed PHP tool. In this case, the procedure is manually started after each single data downloading.

The CO_2 soil flux measurements are acquired using an accumulation chamber provided by Thearen S.r.l (https://thearen.com/). The permanent stations have a no-stationary flux chamber and are equipped with an infrared analyser measuring CO_2 concentrations ($g \cdot m^{-2} \cdot d^{-1}$) in a time frame of three minutes. A single CO_2 flux measure is returned each hour already corrected for pressure (mbar) and temperature (C°) recorded inside the chamber. Soil temperature and humidity (%) and meteorological parameters (atmospheric pressure, temperature, humidity, rain, wind speed and

308   direction) are acquired concurrently. Data are sent to the head company server-cloud through a

309   dedicated modem with automatic data transmission. Data are acquired daily by the INGV acquisition

310   centre through an ad-hoc server to server link using an internal INGV-VPN (Virtual Private Network)

311   connection. Data provided in csv format, are then daily automatically inserted into the MUDA

312   database by using an ad-hoc developed PHP tool.

313

314   The Seismic data are acquired by selected stations of the Italian National Seismic Network

315   (RSN, https://eida.ingv.it/it/networks/network/IV) and the multiparametric network of Northern Italy

316   (PDnet, https://eida.ingv.it/it/networks/network/ZO) placed near the water well used for

317   hydrogeochemical data. Recorded data are codified following the international standard commonly

318   used by the seismological community, namely the FDSN (https://www.fdsn.org/) network-station

319   code and SEED (Standard for the Exchange of Earthquake Data,

320   http://www.fdsn.org/seed_manual/SEEDManual_V2.4.pdf) format supported by European

321   Integrated Data Archive, EIDA (https://eida.ingv.it/it/) and maintained by the FDSN. Data are

322   transmitted by different technologies (LTE, satellite, etc.) to the INGV Milano acquisition centre

323   where they are archived through a Seiscomp4 (https://www.seiscomp.de/doc/apps/seedlink.html)

324   client to improve the SeedLink real time data acquisition protocol. Data are archived in the standard

325   binary miniSEED format (http://ds.iris.edu/ds/nodes/dmc/data/formats/miniseed) and organized in a

326   structured archive. Seismic data are pre-processed every night considering the 24 hours of all

327   miniSEED files recorded by stations on the previous day and then checked for quality before being

328   automatically included in the MUDA database by using an ad-hoc developed PHP tool.

329   In dependence of the adopted sampling rate (i.e. 100 Hz for seismometers and 200 Hz for

330   accelerometers) the amount of continuous data stream per day, relative to a single channel at each

331   single station, ranges between 6 and 10 Mbyte for seismometers and between 15 and 20 Mbyte for

332   accelerometers. Considering many seismic stations, the result is a total daily archive in the order of

333   Gigabytes, not easy to organize in the framework of a quasi-real time data distribution provided by a

334 thematic web portal. In this framework, also considering the sampling rate of the other

335 multiparametric instrumentation (i.e. spanning from one record per minute to one record every four

336 hours), the continuous seismic data streams are processed in order to conform the contents to the web

337 portal requirements before inclusion in the MUDA database. In particular, every night at 2 a.m.

338 miniSEED files relative to the 24-hour recordings of the previous day are selected at each station and

339 processed by using an ad-hoc procedure developed by merging the Bash and SAC (Seismic Analysis

340 Code, https://ds.iris.edu/files/sac-manual/) scripting languages.

341 The processing scheme starts by downloading at each single recording station 24 hours of miniSEED

342 files; data are then separated into 288 sub-windows, each one with length of 5 minutes starting from

343 the origin time of each single miniSEED file (usually corresponding to the 00:00:00 UTC if the station

344 works well). Then, for each 5-minute windows, raw data recorded in counts are converted to the

345 proper unit of measurements (cm/s for seismometers and gal for accelerometers) and the sensor

346 response curves are removed by deconvolution and finally filtered using a 4th order Butterworth filter

347 in the range 0.1 - 20 Hz. For each single sub-window relative to a specific channel recorded by a

348 specific station, the RMS (Root Mean Square, e.g. Goldstain et al., 2003), the maximum ground

349 shaking in terms of velocity (cm/s), the mean amplitude value of the whole FFT (cm/s/Hz) (Fast

350 Fourier Transform, e.g. Bormann 2012) and the maximum amplitude of the FFT for frequency

351 interval spanning from 0.1 Hz to 20 Hz, are calculated, providing for each parameter 288 values per

352 day, corresponding to the daily upload of hydrogeochemical and meteorological data. In particular,

353 the RMS is calculated for the entire time windows using the following equation:

354

355 $$x_{RMS} = \sqrt{[1/n \, (x1^2 + x2^2 + ... + xn^2 \,)]} \qquad (1)$$

356

357 where x is the amplitude of the single sample, and n the number of samples of the trace considered.

358 Daily time series of RMS, PGV, FFT-mean and FFT(f) are finally uploaded into the MUDA database

359 using an ad-hoc developed PHP tool.

361

4.2 Data availability and dissemination

363

MUDA publishes and shares the available data recorded at each site through a specific web interface developed in PHP (https://www.php.net/) to easily and effectively interact with MUDA SQL database, and using a responsive design in HTML5, capable of adapting automatically to any device on which it is displayed (i.e. PC, tablet, smartphone, etc.). As a final step, the data publication required assigning a regular DOI associated to the DB and provided by INGV data management office through a standard procedure. The final DOI of MUDA is https://doi.org/10.13127/SD/ku7Xm12Yy9. Data have been licensed using the Creative Commons License CC BY 4.0. MUDA web portal publishes multiparameter data daily and updated to the previous day. It offers the chance to view and download dynamic time series for all available data and for different time periods, up to a maximum of 30 days. In reference to longer periods, an e-mail request can be sent to: muda@ingv.it.

The web portal has a main page showing an interactive map of Northern and Central Italy, as at present MUDA acquires data from automatic stations located in this part of the Country, where the multiparametric stations are indicated by triangles with pop-ups showing the main features (i.e. coordinates and available instrumentation) of the target site, including the direct access to the dynamic data viewing (Figure 3) and to the single station page (Figure 4). The home page on the top right corner shows a pop-up menu with selectable thematic layers including the reference seismic hazard map of the national territory in terms of peak ground acceleration (MPS04 working group, http://zonesismiche.mi.ingv.it/, Stucchi et al., 2011), the seismogenic areas and the active faults taken from the Database of Individual Seismogenic Sources database (DISS, https://diss.ingv.it/, DISS working group 2021), recent (https://terremoti.ingv.it/) and historical (https://emidius.mi.ingv.it/CPTI15-DBMI15/) seismicity bulletins, and the location of seismic stations of the National Seismic Network (RSN, https://eida.ingv.it/it/networks/network/IV) managed by INGV.

387   The *View & Download DATA* web page, accessible from the horizontal tool bar of the home

388   page, opens the dynamic data viewing (Figure 3). Users can select for each multiparameter site the

389   time series to be displayed backwards in time (i.e. 1 day, 7 days, 15 days, 30 days) starting from a

390   selected date. Once the site and period have been chosen, the available data automatically appear

391   synchronised with respect to UTC (Coordinated Universal Time). From top to bottom, these are:

392   hydrogeochemical data from well or spring sensors showing water temperature (°C), electrical

393   conductivity (µS/cm) and the value of the water column (m) above the sensors; meteorological data

394   showing air temperature (°C) and rainfall (mm); seismometric data showing the RMS, the maximum

395   ground velocity values (cm/s), the average FFT amplitude values, the Fourier spectrum values for

396   frequency bands selected in the interval 0.1 - 20 Hz; Radon gas emissions (Bq/m^3) and soil CO_2 flux

397   ($g \cdot m^{-2} \cdot d^{-1}$). All interactive graphs can be zoomed with the left mouse button and they enable selecting

398   individual functions using pop-up layers. In each graph, in the top right-hand corner, it is possible to

399   view the individual image in full screen and download the selected data in csv (Comma Separated

400   Values) format as well as the images in pdf (Portable Document Format), png (Portable Network

401   Graphic), jpeg (Joint Photographic Experts Group), svg (Scalable Vector Graphics) formats. The last

402   selectable item, on the right of this page, gives the possibility of viewing a single parameter, for a

403   more detailed observation.

404   A further topic of the MUDA web portal is the single station web page (i.e. link *STATIONS*),

405   also reachable from the horizontal tool bar. This web page is designed to provide a first and general

406   geophysical and geochemical characterization of each multiparametric site. In particular, each single

407   station web page shows, on the left, a thematic map indicating the location of the monitoring site.

408   Below the map, the two links provide a geological and morphological setting of the area. For each

409   recording site, a portion selected from the geological map at a 1:100,000 scale (Società Geologica

410   Italiana, http://www.isprambiente.gov.it/it/cartografia/) is provided, with topographic base at

411   1:25,000   scale   (Istituto   Geografico   Militare,

412   http://www.igmi.org/prodotti/cartografia/carte_topografiche/). Concerning morphology, for each

413 recording site, a topographic map (i.e. Slope and Ridge) is proposed by considering the available

414 digital elevation model (ASTER GDEM with a cell size of 10 m,

415 https://www.earthdata.nasa.gov/news/new-aster-gdem). Starting from the processed DEM, the slope

416 map was constructed with three topographic classes (0°–15°, 15°-30°, and >30°), considering the

417 break values defined in the current Italian seismic code (NTC, 2018). The ridgelines were extracted

418 using the Topographic Position Index (TPI) algorithm (Weiss, 2001; Pessina and Fiorini, 2014). On

419 the right, the web page shows thematic tables relative to the installed instrumentation. At each site,

420 besides the general information on coordinates and technical features of the instruments, a

421 geophysical characterization of the site is also provided in terms of polarized horizontal to vertical

422 spectral ratio (HVSR) on ambient noise (Nakamura, 1989) and each single log performed in the wells

423 regarding water electrical conductivity and temperature as a function of the available stratigraphy

424 together with the main features of monitored well or spring. Finally, in each station web page, graphs

425 relative to the whole hydrogeochemical time series are also downloadable.

426

427 **5 Data Records**

428

429 At present (i.e. March 31, 2024), MUDA includes data from 25 multiparametric sites (Table

430 1) located in Northern and Central Italy (Figure 2), both already monitored by permanent INGV

431 infrastructures or installed in the framework of recent INGV research projects. It is worth mentioning

432 that not all multiparametric sites are characterized by homogeneous multiparametric instrumentation

433 (Figure 6). In any case, all available data are always sent in real time to the INGV acquisition centres.

434 In particular, concerning seismic data, the multiparametric sites include 7 stations belonging to the

435 permanent National Seismic Network (RSN, https://eida.ingv.it/it/networks/network/IV) and 12

436 stations belonging to the temporary multiparametric network of Northern Italy (PDnet, FDSN code

437 ZO, https://eida.ingv.it/it/networks/network/ZO), installed in the framework of the INGV Dynamic

438 Planet S2-project. These sites are located in Northern Italy, around the Lake Garda, at the southern

439   limit of the Eastern Italian Alps and in the central portion of the Po Plain (Figure 2). Two further

440   seismic stations (PDN11, PDN12, table 1) have recently been installed in the framework of the INGV

441   Dynamic Planet GEMME (Integrated Geological, gEophysical and geocheMical approaches for 3D

442   Modelling of complex seismic site Effects) project, in Norcia basin (Apennine chain in central Italy)

443   and its surroundings (Figure 2). Finally, one seismic station (PDN10, table 1) has been installed in

444   cooperation with the Dynamic Planet PROMUD (Definition of a multidisciplinary monitoring

445   PROtocol for MUD volcanoes) project, in the Salse di Nirano Reserve (Italian Northern Apennines,

446   Figure 2).

447   In general, seismic stations are equipped with high dynamic 24-bit digital recording systems

448   coupled to enlarged (5s owner period) or broadband (120s owner period) seismometers. In particular,

449   at Oppeano multiparametric site (Table 1), borehole instrumentation is installed at 150 m depth. Even

450   if in some cases accelerometer sensors are coupled to the target seismometer (velocimeter), MUDA

451   includes only seismometric data due to their higher sensitivity and best resolution with respect to

452   possible occurrences of natural phenomena such as micro seismicity, local weak motion earthquake

453   occurrences and/or teleseisms or environmental modifications (i.e. landslides, low atmospheric

454   pressure, tides etc.).

455   Hydrogeochemical data are recorded in all 25 multiparametric sites (Table 1), at both wells

456   and springs set up in the framework of INGV Dynamic Planet projects (S2 and GEMME) and INGV

457   Multiparametric Networks or the Rebuilt central Italy, DL50 project. The Toppo site (Table 1),

458   installed   in   the   eastern   Alps   in   the   framework   of   the   Eccsel   Eric   consortium

459   (https://www.eccsel.org/), is managed by OGS (National Institute of Oceanography and Applied

460   geophysics, https://www.ogs.it/en) in cooperation with the University of Ferrara (Department of

461   Physics and Earth Science, http://fst.unife.it/en) and the INGV. At present, data included in MUDA

462   are recorded at 22 wells and 3 springs (Recoaro, Recoaro1, Feltre, see table 2). In general, wells have

463   depths ranging from a few meters (< 10 m) to a maximum of 300 m for Toppo and Mirandola sites

464   (Table 2). The instrumented wells have a mean depth between 5 and 150 m. Monitored sites are

465 mainly characterized by cold waters whose average temperatures range from 10.3 to 17.4 °C, except

466 for TRIPONZO site that owns thermal water (~ 30 °C; Table 2). A wide variety of water electrical

467 conductivity values (~ 130-88000 µS/cm; Table 2) are illustrative of heterogeneous compositions and

468 salt contents. Information on the presence of borehole pump (Table 2), frequency and intensity of

469 water pumping were carefully collected from well owners. Water level, temperature and electrical

470 conductivity changes are observed because of pumping for water chemical analysis (e.g., Balconi) or

471 irrigation purposes (e.g., Norcia) or functioning of spa (e.g., Triponzo). These anthropogenic

472 variations must be accounted for when analysing groundwater data. A comprehensive example of

473 data-processing able to recognize in groundwater time series both natural phenomena and

474 anthropogenic noise signals is reported in Ferrari et al. (2024) for the site of Balconi.

475 All sites monitored by hydrogeochemical instrumentation are also equipped with a

476 meteorological station able to capture the main atmospheric variations.

477 Four sites (i.e. Montelungo, Bondo, Norcia, Triponzo, table 1) are currently equipped with

478 instrumentation able to record the Radon concentration in the air. Sensors for Radon monitoring are

479 part of the IRON network (Italian Radon mOnitoring Network, https://ingv.it/monitoraggio-e-

480 infrastrutture/reti-di-monitoraggio/l-ingv-e-le-sue-reti/iron) of INGV. Finally, just one site (i.e.

481 Nirano, table 1) is equipped with instrumentation for Carbon Dioxide (CO_2) soil flux measurements.

482

483 In general, the multiparametric sites show co-located instrumentation, with a few exceptions

484 due to logistic difficulties during the site installation or other technical problems (e.g. sites with a

485 very high level of background seismic ambient noise or working pump installed in well). In all cases,

486 the reference seismic station is installed in the same geological, morphological and hydrogeological

487 context as the other instruments, possibly co-located or at least in the proximity. Hydrogeochemical

488 stations installed in a narrow area (e.g., Bulgarelli, Medolla, Mirandola and Secchia sites, table 2)

489 might refer to the same seismic station.

490

5.1 Data quality check

In order to verify the completeness and correctness of the recorded data, we carried out several checks.

Concerning seismic data included in MUDA, the results of the processing procedure to produce 5 minutes interval data are verified to check the capacity of the proposed processing scheme to represent a real marker to detect earthquakes or environmental phenomena. Figure 7 reports an exhaustive example at the Oppeano site for events recorded by the seismic station on December 29, 2020. Figure 7 shows in the panel *a* (top) the occurrences of subsequent events in a narrow time window spanning from 2020/12/29 14:02:40 to 15:36:57 UTC. The first evident transient is related to the regional M_w=6.3 Croatia earthquake on 2020/12/29 at 12:19:54 UTC (https://terremoti.ingv.it/event/25870121). A few hours later, a small sequence of three local weak motion was recorded 12 km South West of Oppeano and localised by the INGV bulletin at 2020/12/19 14:02:40, 14:44:51 and 15:36:47 UTC with magnitudes of M_L=3.4, M_L=2.8 and M_w=3.9, respectively (https://terremoti.ingv.it/event/25871441). In the bottom of panel *a* the results of our detector procedure in terms of FFT interval is shown for the 288 data points of the 2020/12/29. It is evident how all transients have been clearly recognized by marked peaks: in particular, the regional event, occurring about 400 km East of the Oppeano well highlights a notable contribution at low frequency, showing a clear peak for the FFT around 0.1 Hz. On the contrary, the local seismicity is well described by peaks detected at higher frequency content, in particular ranging from 1 to 10 Hz. In this case, it is worth noting how the high frequency content of FFTs also highlight variations in ambient noise level between night and day. In the panel *b* of figure 7, the results of the detection procedure are presented in terms of relative RMS, ground motion velocity and averaged FFTs (from top to bottom).

In order to publish reliable results, all continuous seismic data streams for all seismic stations are checked daily for quality by the interoperability between MUDA and ISMDq (INGV Strong Motion Data quality, http://ismd.mi.ingv.it, Massa et al., 2022). In this way all seismic stations

included in MUDA are checked for gaps (%), availability (%) and ambient noise level variation in terms of PSD (Power Spectral Density) and PDF (Probability Density Function), in dB, as calculated by McNamara and Buland (2004). Through ISMDq, it is possible to build temporal time series with a maximum time length of up to 2 years for all stations included in MUDA in order to check at first the correct functioning of the stations, the accuracy of used metadata, daily and seasonal variations of ambient noise level and transient or permanent anthropic disturbances. In particular, in case of failure in data transmission, the continuous monitoring of data gaps and availability allow us to retrieve data directly from station memories thereby avoiding important gaps in the data.

Hydrogeochemical and geochemical data are checked daily for availability and gaps usually due to a temporary lack of data transmission platforms (i.e. cellular line or satellite), in particular during rainy and stormy days or more rarely due to malfunctioning of the instrumentation. In the first case, the recorders, thanks to their internal memory and datalogging capacity, are able to archive data up to a maximum of 30 days. If needed, the recovery of data is possible through a manual download. Subsequently data are uploaded into the MUDA database by calling the same ad-hoc developed tools for populating the database for each parameter, with appropriate flags. In some cases, water level time series show unusual abrupt peaks (i.e. spurious spikes that are filtered) due to some problems during the compensation of atmospheric pressure performed by the recording system in order to obtain the correct values of water level: in general, misalignments in pressure compensation lead to wrong water level values, usually with differences of ~ 10 m, as a consequence of the measured atmospheric pressure usually around or slightly above 1000 mbar, considering that all the stations are within a few hundred meters above sea level.

Other data included in MUDA (i.e. meteorological, Radon, CO_2 flux) do not need particular processing. In any case, for all meteorological, Radon and CO_2 measurements, data are always checked for gaps and possible spurious peaks that are deleted. In particular, meteorological data regarding the pluviometry are archived and uploaded into MUDA as a single sample recorded each minute, or even better, in some cases, at each individual movement of the rain gauge's tipping bucket

(0.2 mm every time). In these cases, before publishing the rain values on the web site, data are cumulated in intervals of 1 hour directly in the SQL query made by the web portal, in order to better highlight heavy storms or other particular meteorological phenomena.

6 Multiparametric monitoring

In this section, some examples of comparison among multiparametric data are presented and discussed in the framework of their possible applications for research and services devoted to natural hazard risk reduction.

An interesting example of multiparametric monitoring, concerning groundwater level variation presumably related to large landslide phenomena has been collected at the Bondo (Table 1) site and aquifer (Lake Garda area, Figure 2), where on the November 1, 2023, the water column above the sensor in the well abruptly increased by ~ 20 m. This significant modification, also combined with the diminishing temperature and electrical conductivity (Figure 8, panel *a*), happened as a consequence of 2 days of intense rainfall with measured values of precipitation up to 400 mm in a narrow area surrounding Bondo. It is important to highlight that the stratigraphy below Bondo is mostly made of fractured-carsified limestones belonging to the Dolomia Principale formation (Upper Triassic). To explain such a notable groundwater level variation, additional and contemporary natural phenomena should be hypothesized; on the base of the information provided by the local media, in the same period the area was affected by diffuse landslides. In particular, between October 31 and November 1, 2023, a clear seismic transient (Figure 8, panel *b*) was recorded on all 3 components of ZO.PDN3 station (Table 2), characterized by very long duration (i.e. some hours), higher amplitudes with respect to the local ambient noise level (i.e. the Peak Ground Velocity, PGV was equal to 0.01 cm/s, comparable to a local earthquake with magnitude ranging from 2.5 and 3.0), prevalent high frequency content (~ 5-30 Hz) and a strong polarisation with preferential amplification of motion along the NS direction (Figure 8, panel *c*). In this case, the recorded transient at ZO.PDN3 could in

569 fact be attributable to local and diffuse landslides that could have modified the volume and/or the

570 extent of the aquifer and eventually the water flow infiltration and circulation through the rock

571 fractures by influencing the water level and leading the aquifer to be more sensitive to meteorological

572 events.

573   Meteorological events, in particular the intense rainfall period, also seem to have a strong

574 influence on Radon emission measurements, usually adopted as a possible marker in case of a tectonic

575 event. An example can be observed considering the complete Radon time series at the Bondo site

576 where data highlight a positive correlation with the seasonality, with increasing values in summer and

577 decreasing values in winter, following the trend of both atmospheric pressure and temperature. At

578 least during the monitored period, at the Bondo site no correlation with local seismicity appears to be

579 noticeable, while clear correlations between Radon outliers and the rainfall period are evident (Figure

580 9, panel *a*). It is worth mentioning how not all Radon sensors show the same behaviour with respect

581 to the season. At the Montelungo site (Table 1), for instance, data show a complete anti-correlation

582 with the seasons (Figure 9, panel *b*), with lower values in summer and higher values in winter,

583 probably as a consequence of the different local geological and morphological setting.

584   A further example regards the CO_2 flux variation, measured at the Nirano site (Table 1) in

585 October 2023 (Figure 10, panel *a*) during an intense period of weak motion earthquakes localized

586 very close to ZO.PDN10 station, installed in the area of the Salse di Nirano regional park. Starting

587 from June 2023, the area of Nirano showed an increase in the local seismicity. In the period

588 2023/06/01 to 2023/11/15, 32 earthquakes with local magnitude (M_L) in the range 2.0-3.5 were

589 recorded with a maximum epicentral distance from Nirano of 30 km. In particular, the strong events

590 with M_L=3.5 occurred on October 30, 2023 (04:25:53 UTC). Considering the CO_2 time series

591 recorded at Nirano and a time period spanning from October 15 to November 15, 2023, it is possible

592 to highlight the presence of many CO_2 data points with values exceeding the limit of +1 standard

593 deviation (Figure 10, panel *b*), with respect to the average values of the period. Many outliers were

594 recorded just before and also soon after the M_L=3.5 target earthquake. It worth noting that this

595 evidence should be carefully evaluated also considering other parameters (for instance, atmospheric

596 pressure, soil moisture and temperature), even though no relevant rainfall episodes occurred in that

597 period.

598 Further case studies concern the correlation between meteorological (i.e. temperature and

599 rainfall) and groundwater parameters. Understanding water level fluctuation patterns is one of the

600 pillars for designing adaptive management practices that can mitigate the impacts of extreme water

601 levels on infrastructure and associated economic activities (e.g. Gerten et al., 2013, Alley et al., 2002,

602 Taylor et al., 2009; Russo and Lall, 2017). Groundwater recharge is difficult to estimate, especially

603 in fractured aquifers, because of the spatial variability of the soil properties and because of the lack

604 of data at basin scale. A possible solution consists in inferring recharge directly from the observation

605 in boreholes (Guillaumot et al., 2022), even if the direct measures in wells overlook the impact of

606 lateral groundwater redistribution in the aquifer. When evaluating the effect of exogenous parameters

607 on groundwaters, rainfall is the main factor in promptly influencing all monitored groundwater

608 parameters (e.g. Mancini et al., 2022, Guillaumot et al., 2022), with a variable aquifer response with

609 respect comparable amounts of precipitation in the same period. Figure 11 shows an example of

610 groundwater recordings related to the meteorological event of October 2023 at Volargne and Fonte

611 sites (table 1). It is worth noting how in the first site (Figure 11, panel *a*) a gradual and moderate rise

612 in water level is contrasted by a faster and larger (less than 2 hours) increase in water level at the

613 Fonte site (Figure 11, panel *b*), which shows an intense influence of the rainfall, also proved by the

614 extremely variable temperature and conductivity records not observed in the other sites (Ferrari et al.,

615 2024). The light grey box in Figure 11 highlights another instant response of Fonte groundwater to

616 precipitation which is even more sharper than the one described above and also involves electrical

617 conductivity decrease and temperature increase.

618 The atmospheric temperature is moreover proven to affect groundwater temperature,

619 especially in aquifers down to ~ 20 m depth (e.g. Lee and Hahn, 2006, 2021; Taylor and Stefan, 2009;

620 Menberg et al., 2014). Monitoring sites having at least 1 year of recordings are taken into account to

analyse groundwater temperature seasonal oscillations and correlations to air temperature. In our case, the absence of seasonality is detected at the Bondo, Montelungo and Volargne sites (Table 1) where the constant groundwater temperatures could be explained by the aquifer depth (~ 50 m). In other cases, such as the Casaglia site (Table 1), despite the depth of aquifer of a few meters below ground level, the relevant water (~ 40 m) column above the hydrogeochemical sensor dampened possible temperature fluctuations (Bucci et al., 2020; Egidio et al., 2022). On the contrary, at the Balconi site (Table1), despite the aquifer depth is greater than 50 m, a nearly seasonal variation characterized by maximum values reached in summer and minima in winter, is observed, in agreement with the measured air temperature periodicity (Ferrari et al., 2024). However, it should be evaluated whether this temperature variation in specific seasons is directly attributable to meteorological reasons or to anthropogenic causes, due to intense irrigation occurring in the area of Balconi during the most dry and hot months of the year.

7 Usage Notes and conclusions

The technical validation allowed us to obtain a reliable and homogenous dataset of continuous multiparametric time series and associated metadata. For hydrogeochemical, meteorological, Radon and CO_2, data are published in a raw format after a pre-processing whose main scope was just to detect gaps and spurious peaks to be deleted from the time series. Seismic data are published after applying a 5-minute resampling to the raw miniseed 24-hour continuous data and then by converting the velocity ground motion (cm/s) in RMS and FFT discrete time series. The raw seismic waveforms are however downloadable from the EIDA-Italia webservice (https://eida.ingv.it/it/).

For the first time, at least in Italy, high frequency and continuous multiparametric data are dynamically updated daily and published soon after for end users. Data can be used for different purposes, ranging from i) information regarding environmental and meteorological temporal trends with respect the global climate change problematic; ii) details on local aquifer features and seismicity;

iii) recommendations for the civil protection; iv) multiparametric geophysical, environmental and geochemical data for research studies. In particular, all seismic stations included in MUDA-db with code ZO (PDnet, https://eida.ingv.it/it/networks/network/ZO) contribute with the national seismic monitoring by sharing a continuous data stream in real time to the INGV National Seismic Network (https://eida.ingv.it/it/networks/network/IV). In addition, the dense ZO network installed around Lake Garda contribute significantly to improving the minimum magnitude threshold detection of the area as reported in Ferrari et al. (2024).

Seismic data, together with all geological, morphological and geophysical information collected at each site included in MUDA, can moreover be used to investigate the site response in terms of seismic amplification, in particular for sites installed in the central part of the Po Plain, a deep basin characterized by a significant thickness of incoherent alluvial deposits. Seismic events recorded at each station can also be used for local investigations into the micro seismicity of the area, seismic source recognition or to improve the available seismic velocity models at a local scale.

Hydrogeochemical and geochemical data will be used in the framework of a recent agreement between the National Institute of Geophysics and Volcanology (INGV) and the National System for Environmental Protection (SNPA, comprising the Regional Environmental Protection Agencies - ARPA and ISPRA), aimed at gathering information on seismic activity and aquifer/spring status from various acquisition sources, in some cases reaching a near real time monitoring through the SINAnet facility (https://www.snpambiente.it/attivita/sistema-informativo-nazionale-ambientale/).

In general, the multiparametric monitoring is the basis by which to understand and identify possible seismic precursors, an objective not yet achieved in earthquake studies. In particular, the short-term earthquake forecasting, remains elusive and largely unattained. An effective solution for such a major issue might be found, in the future, in systematic high frequency and continuous measurements with multiparametric networks operating over the long term. Owing to the influx from deep crustal fluids in active tectonic areas, groundwater monitoring may especially be considered a

672 fundamental tool for investigating pre-seismic signals of rocks undergoing accelerated strain (e.g.

673 King, 1986; Skelton, A. et al. 2014, Barberio et al., 2017).

674

675 **8 Data Availability**

676

677 Data and metadata presented and described in this manuscript can be accessed

678 under https://doi.org/10.13127/muda (Massa et al., 2023).

679

680 **9 Code Availability**

681

682 All the procedures to acquire and process data coming from multiparametric remote stations

683 have been specifically developed for the MUDA project in Bash scripting language, Python and PHP

684 language, using, when necessary, proprietary API taken from the manufacturers of the installed

685 remote instrumentation, as detailed in the text. Seismic data are acquired and archived through a

686 Seiscomp4 (https://www.seiscomp.de/doc/apps/seedlink.html) client, thereby improving the

687 SeedLink real time data acquisition protocol. Some processing steps on the seismic data are

688 undertaken using the Seismic Analysis Code (SAC,

689 https://ds.iris.edu/ds/nodes/dmc/software/downloads/sac/), a software designed for both real time and

690 off-line seismological analyses of time series data. The MUDA database is developed with MySQL

691 open source software. The MUDA web portal is developed in PHP and HTML5 languages, and all

692 data are published under the Creative Commons License CC BY 4.0 licence.

693

694

695

696

697

698 **Team list**

699

700 MUDA working group is at present composed by the main authors and:

701 Marino Domenico Barberio [4], Gianfranco Tamburello [5], Gioia Capelli Ghioldi [5], Santi Mirenna [1],

702 Ezio D'Alema [1], Anna Figlioli [1], Pellegrino Moretti [1], Claudio Ventura Bordenca [1], Fabio

703 Varchetta [1], Antonio Piersanti [4], Valentina Cannelli [4], Gianfranco Galli G. [4], Rodolfo Puglia [1].

704

705 [1] National Institute of Geophysics and Volcanology (INGV), Milano department, Italy

706 [4] National Institute of Geophysics and Volcanology (INGV), Roma1 department, Roma, Italy

707 [5] National Institute of Geophysics and Volcanology (INGV), Bologna department, Italy

708

709 **Author contributions**

710

711 This study started from an original idea by MM and ALR. MM, ALR, EF and SL contributed

712 to all phases of site installations, data acquisition, processing and archiving. DS developed MySQL-

713 Db and the associated web page, as well as the procedures to upload data into MUDA-db. SL and EF

714 contributed to organising the technical data sheet related to each multiparametric site now available

715 at each single station web page. MM developed the procedures for multiparametric data pre-

716 processing and seismic data post processing. All authors participated in the preparation of the

717 manuscript draft and in the phases of revision.

718

719 **Competing Interests: The authors declare no competing interests.**

720

721

722

723

747

748

749 **References**

750

751 Aiuppa, A., Federico, C., Giudice, G., Gurrieri, S. Chemical mapping of a fumarolic field: La Fossa

752 Crater, Vulcano Island (Aeolian Islands, Italy). Geophys. Res. Lett. 32 (13), 1-4 (2005).

753

754 Allard, P., Burton, M., Murè F., Spectroscopic evidence for a lava fountain driven by previously

755 accumulated magmatic gas. Nature 433, 407-410, doi:10.1038/nature03246 (2005).

756

757 Alley, W.M., Healy, R.W., LaBaugh, J.W., Reilly, T.E., Flow and storage in groundwater systems.

758 Science 296 (5575), 1985-90, doi: 10.1126/science.1067123 (2002).

759

760 Barberio, M.D., Barbieri, M., Billi, A., Doglioni, C., Petitta, M., Hydrogeochemical changes before

761 and during the 2016 Amatrice Norcia seismic sequence (central Italy). Sci. Rep. UK 7:11735, 1-12.

762 doi:10.1038/s41598-017-11990-8 (2017).

763

764 Battaglia, M., Murray, M.H., Serpelloni, E., Bürgmann, R., The Adriatic region: an in dependent

765 microplate within the Africa-Eurasia collision zone. Geophys. Res. Lett. 31, L09605,

766 doi:10.1029/2004GL019723 (2004).

767

768 Bigi, G., Costantino, D., Parotto, M., Sartori, R., Scandone, P., Structural Model of Italy. Firenze,

769 Società Elaborazioni Cartografiche (S.EL.CA.). Consiglio Nazionale Delle Ricerche Progetto

770 Finalizzato Geodinamica, Scala 1:500.000, 9 Fogli (1990).

771

772 Bonini, M., Elliptical mud volcano caldera as stress indicator in an active compressional setting

773 (Nirano, Pede-Apennine margin, northern Italy). Geology 36, 131-134, doi:10.1130/G24158A.1

774 (2008).

775

776   Bormann, P., (Editor) New manual of seismological observatory practice (NMSOP-2), IASPEI, GFZ

777   German Research Centre for Geosciences, Potsdam, https://gfzpublic.gfz-potsdam.de/ (see data and

778   resources), doi:10.2312/GFZ.NMSOP-2 (2012).

779

780   Bräuer, K., Kämpf, H., Strauch, G., Weise, S.M., Isotopic evidence (^{3}He/^{4}He, $^{13}C_{CO2}$) of fluid-

781   triggered intraplate seismicity. J. Geophys. Res. 108(B2), 1-11, doi:10.1029/2002JB002077 (2003).

782

783   Brozzetti, F., Lavecchia, G., Seismicity and related extensional stress field: the case of the Norcia

784   Seismic Zone (Central Italy). Annales Tectonicae 8 (1), 36-57 (1994).

785

786   Bucci, A., Lasagna, M., De Luca, D.A., Acquaotta, F., Barbero, D., Fratianni, S., Time series analysis

787   of underground temperature and evaluation of thermal properties in a test site of the Po plain (NW

788   Italy). Environ. Earth Sci. 79,185, doi:10.1007/s12665-020-08920-9 (2020).

789

790   Burton, M.R., Caltabiano, T., Murè, F., Salerno, G.G., Randazzo, D., SO2 flux from Stromboli during

791   the 2007 eruption: results from the FLAME network and traverse measurements. J. Volcanol.

792   Geotherm. Res. doi:10.1016/j.jvolgeores.2008.11.025 (2009).

793

794   Burrato, P., Vannoli, P., Fracassi, U., Basili, R., Valensise, G., Is blind faulting truly invisible?

795   Tectonic-controlled drainage evolution in the epicentral area of the May 2012, Emilia-Romagna

796   earthquake sequence (northern Italy). Annals of Geophysics 55, 4, 525-531 (2012).

797

798   Buttitta, D., Caracausi, A., Chiaraluce, L., Favara, R., Morticelli, M.G., Sulli, A., Continental

799   degassing of helium in an active tectonic setting (northern Italy): the role of seismicity. Scientific

800   Reports 10, Article number:162 (2020).

801

802   Cannelli, V., Piersanti, A., Galli, G., Melini, D., Italian Radon mOnitoring Network (IRON): A

803   permanent network for near real-time monitoring of soil radon emission in Italy. Annals of geophysics

804   4/61, 10.4401/ag-7604 (2018).

805

806   Carapezza, M.L, Inguaggiato, S., Brusca, L., Longo, M., Geochemical precursors of Stromboli 2002–

807   2003 eruptive events. Geophys Res Lett 31(7):10.1029/2004GL019614 (2004).

808

809   Castaldini, D., Valdati, J., Ilies, D.C., Chiriac, C., Bertogna, I., Geo-tourist map of the natural reserve

810   of Salse di Nirano (Modena Apennines, Northern Italy). Italian Journal of Quaternary Sciences 18(1),

811   245-255 (2005).

812

813   Cicerone, R.D., Ebel, J.E., Britton, J., A systematic compilation of earthquake precursors.

814   Tectonophysics 476, 371-396, doi:10.1016/j.tecto.2009.06.008 (2009).

815

816   Chiarabba, C., Piccinini, D., De Gori, P., Velocity and attenuation tomography of the Umbria Marche

817   1997 fault system: Evidence of a fluid-governed seismic sequence. Tectonophysics 476, 73-84,

818   doi:10.1016/j.tecto.2009.04.004 (2009).

819

820   Chiaraluce, L., Collettini, C., Cattaneo, M., Monachesi, G., The shallow boreholes at The

821   AltotiBerina near fault Observatory (TABOO; northern Apennines of Italy), Volume 17, Scientific

822   Drilling, 17, 31-35, https://doi.org/10.5194/sd-17-31-2014 (2014).

823

824   Chiaraluce, L., Di Stefano, R., Tinti, E., Scognamiglio, L., Michele, M., Casarotti, E., Cattaneo, M.,

825   De Gori, P., Chiarabba, C., Monachesi, G., Lombardi, A., Valoroso, L., Latorre, D., Marzorati, S.

826   The 2016 Central Italy Seismic Sequence: A First Look at the Mainshocks, Aftershocks, and Source

827   Models. Seismological Research Letters 88 (3), 757–771 (2017).

828

829 Chiodini, G., Cioni, R., Guidi, M., Raco, B., Marini, L., Soil CO2 flux measurements in volcanic and

830 geothermal areas. Appl. Geochem. 13, 543-552 (1998).

831

832 Chiodini, G., Cardellini, C., Di Luccio, F., Selva, J., Frondini, F., Caliro, S., Rosiello, A., Beddini, G.,

833 Ventura, G., Correlation between tectonic CO_2 Earth degassing and seismicity is revealed by a 10-

834 year record in the Apennines, Italy. Sci. Adv. 6:eabc2938, 1-7, doi:10.1126/sciadv.abc2938 (2020).

835

836 Comerci, V., Doglioni, C., Italiano, F., Baiocco, F., Barberio, M.D., Caracausi, A., Cuiuli, E., Guerra,

837 M., Infantino, V., Insolvibile, M., Marcaccio, M., Martinelli, G., Menichetti, S., Onorati, G., Petitta,

838 M., Palumbo, V., Peleggi, M., Richieri, F., Scaramella, A., Scotti, E., Testa, M., Towards a national

839 hydrogeochemical monitoring system: a further tool to investigate geological hazards. Misc. INGV

840 49, 1-338 (2019).

841

842 D'Alessandro, A., Scudero, S., Siino, M., Alessandro, G., Mineo, R., Long-term monitoring and

843 characterization of soil radon emission in a seismically active area. Geochem. Geophy. Geosy.

844 21:e2020GC009061, doi:10.1029/2020GC009061 (2020).

845

846 D'Agostino, N., Avallone, A., Cheloni, D., D'Anastasio, E., S Mantenuto, Selvaggi, G., Active

847 tectonics of the Adriatic region from GPS and earthquake slip vectors. Jour. Geophys. Res. 113 (B12),

848 B12413 (2008).

849

850 Danecek, P., Pintore, S., Mazza, S., Mandiello, A., Fares, M., Carluccio, I., ... & Michelini, A., The

851 Italian node of the European integrated data archive. Seismological Society of America, 92(3), 1726-

852 1737, doi:https://doi.org/10.1785/0220200409 (2021).

853

854   Danesi, S., Pondrelli, S., Salimbeni, S., Cavaliere, A., Serpelloni, E., Danacek P., Lovati, S., Massa,

855   M., Active deformation and seismicity in the Southern Alps (Italy): The Montello hill as a case study.

856   Tectonophysics 653, 95-108, doi:10.1016/j.tecto.2015.03.028 (2015).

857

858   De Gregorio, S., Gurrieri, S., Valenza, M., A PTFE membrane for the in situ extraction of dissolved

859   gases in natural waters: Theory and applications. Geochem. Geophys. Geosyst., 6, Q09005,

860   doi:10.1029/2005GC000947 (2005).

861

862   De Gregorio, S., Federico, C., Cappuzzo, S., Favara, R., Giudice, G., Gurrieri, S., Boschi, E., Stress-

863   induced temperature variations in groundwater of the Monferrato area (north-western Italy).

864   Geofluids 12, 142-149, doi:10.1111/j.1468-8123.2011.00348.x (2012).

865

866   De Luca, G., Di Carlo, G., Tallini, M., A record of changes in the Gran Sasso groundwater before,

867   during and after the 2016 Amatrice earthquake, central Italy. Sci. Rep. UK 8:15982, 1-16,

868   doi:10.1038/s41598-018-34444-1 (2018).

869

870   De Matteis, R., Convertito, V., Napolitano, F., Amoroso, O., Terakawa, T., Capuano, P., Pore fluid

871   pressure imaging of the Mt. Pollino region (southern Italy) from earthquake focal mechanisms.

872   Geophys. Res. Lett. 48:e 2021GL094552, doi:10.1029/2021GL094552 (2021).

873

874   Di Luccio, F., Ventura, G., Di Giovambattista, R., Piscini, A., Cinti, F.R., Normal faults and thrusts

875   reactivated by deep fluids: The 6 April 2009 M_w 6.3 L'Aquila earthquake, central Italy. J. Geophys.

876   Res. 115, 1-15, doi:10.1029/2009JB007190 (2010).

877

878   DISS Working Group Database of Individual Seismogenic Sources (DISS), Version 3.3.0: A

879   compilation of potential sources for earthquakes larger than M 5.5 in Italy and surrounding areas.

880   Istituto Nazionale di Geofisica e Vulcanologia (INGV) https://doi.org/10.13127/diss3.3.0 (2021).

881

882   Egidio, E., Mancini, S., De Luca, D.A., Lasagna, M., The Impact of Climate Change on Groundwater

883   Temperature of the Piedmont Po Plain (NW Italy). Water 14:2797, doi:10.3390/w14182797 (2022).

884

885   Ferrari, E., Massa, M., Rizzo, A.L., Lovati, S., Di Michele F., Multiparametric stations for real-time

886   monitoring and long-term assessment of natural hazards. Front. Earth Sci. 12:1412900, doi:

887   10.3389/feart.2024.1412900 (2024).

888

889   The Italian multiparametric network for detection and monitoring of earthquake-related crustal fluids

890   alterations. EGU meeting, Wien, session SM3.4, 14-19 April (2024).

891

892   Gabrielli, S., Akinci, A., Ventura, G., Napolitano, F., Del Pezzo, E., De Siena, L., Fast changes in

893   seismic attenuation of the upper crust due to fracturing and fluid migration: the 2016–2017 Central

894   Italy seismic sequence. Front. Earth Sci. 10:909698, doi: 10.3389/feart.2022.909698 (2022).

895

896   Gabrielli, S., Akinci, A., De Siena, L., Del Pezzo, E., Buttinelli, M., Maesano, F.E., Maffucci, R.,

897   Scattering attenuation images of the control of thrusts and fluid overpressure on the 2016–2017

898   Central   Italy   seismic   sequence.   Geophys.   Res.   Lett.   50:e2023GL103132,

899   doi:10.1029/2023GL103132 (2023).

900

901   Galadini, F., Galli, P., The Holocene paleoearthquakes on the 1915 Avezzano earthquake faults

902   (central Italy): implications for active tectonics in the central Apennines. Tectonophysics 308, 1-2,

903   143-170 (1999).

904

905 Galadini, F., Messina, P., Plio-Quaternary changes of the normal fault architecture in the Central

906 Apennines (Italy). Geodinamica Acta, 321-344, https://doi.org/10.1080/09853111.2001.10510727

907 (2001).

908

909 Galli, P., Galderisi, A., Ilardo, I., Piscitelli, S., Scionti, V., Bellanova, J., & Calzoni, F., Holocene

910 paleoseismology of the Norcia fault system (central Italy). Tectonophysics 745, 154-169,

911 https://doi.org/10.1016/j.tecto.2018.08.008 (2018).

912

913 Galli, P., Galderisi, A., Peronace, E., Giaccio, B., Hajdas, I., Messina, P., Pileggi, D., Polpetta, F. The

914 Awakening of the Dormant Mount Vettore Fault (2016 Central Italy Earthquake, Mw 6.6):

915 Paleoseismic Clues on Its Millennial Silences. Tectonics https://doi.org/10.1029/2018TC005326

916 (2019).

917

918 Gerten, D., Hoff, H., Rockström, J., Jägermeyr, J., Kummu, M., Pastor, A.V., Towards a revised

919 planetary boundary for consumptive freshwater use: role of environmental flow requirements.

920 Environmental Sustainability 5, issue 6, 551-558 (2013).

921

922 Giambastiani, B.M.S., Chiapponi, E., Polo, F., Nespoli, M., Piombo, A., Antonellini, M., Structural

923 control on carbon emissions at the Nirano mud volcanoes – Italy. Marine and Petroleum Geology

924 163, 106771 (2024).

925

926 Goldstein, P., Dodge, D., Firpo, M., Minner, L., SAC2000: Signal processing and analysis tools for

927 seismologists and engineers, Invited contribution to "The IASPEI International Handbook of

928 Earthquake and Engineering Seismology", Edited by WHK Lee, H. Kanamori, P.C. Jennings, and C.

929 Kisslinger, Academic Press, London (2003).

930

931 Gori, F., Barberio, M.D., Hydrogeochemical changes before and during the 2019 Benevento seismic

932 swarm in central-southern Italy. J. Hydrol. 604:127250, 1-10, doi:10.1016/j.jhydrol.2021.127250

933 (2022).

934

935 Guillaumot, L., Longuevergne, L., Marçais, J., Lavenant, N., Bour, O., Frequency domain water table

936 fluctuations reveal impacts of intense rainfall and vadose zone thickness on groundwater recharge.

937 Hydrology and Earth System Sciences 26, issue 22, HESS, 26, 5697–5720,

938 https://doi.org/10.5194/hess-26-5697-2022 (2022).

939

940 Hubbert, M.K., Rubey, W.W., Role of fluid pressure in mechanics of overthrust faulting: mechanics

941 of fluid-filled porous solids and its application to overthrust faulting. Geol. Soc. Am. Bull. 70(2), 115-

942 166, doi:10.1130/0016-7606(1959)70[115:ROFPIM] 2.0.CO;2 (1959).

943

944 Improta, L. and co-Authors Multi-segment rupture of the 2016 Amatrice-Visso-Norcia seismic

945 sequence (central Italy) constrained by the first high-quality catalog of Early Aftershocks. Scientific

946 Reports, 9, 6921 (2019).

947

948 Inguaggiato, S., Vita, F., Rouwet, D., Bobrowski, N., Morici, S., Sollami, A., Geochemical evidence

949 of the renewal of volcanic activity inferred from CO2 soil and SO2 plume fluxes: the 2007 Stromboli

950 eruption (Italy). Bulletin of Volcanology http://dx.doi.org/10.1007/s00445-010-0442-z (2011a).

951

952 Inguaggiato, S., Calderone, L., Inguaggiato, C., Morici, S. and Vita, F., Dissolved CO_2 in natural

953 waters: development of an automated monitoring system and first application to Stromboli volcano

954 (Italy). Annals of Geophysics 54(2), doi: 10.4401/ag-5180 (2011b).

955

956   Italiano, F., Martinelli, G., Rizzo, A., Geochemical evidence of seismogenic-induced anomalies in the

957   dissolved gases of thermal waters: A case study of Umbria (Central Apennines, Italy) both during and

958   after the 1997-1998 seismic swarm. Geochem. Geophy. Geosy. 5(11), 1-11,

959   doi:10.1029/2004GC000720 (2004).

960

961   Italiano, F., Martinelli, G., Nuccio, P.M., Anomalies of mantle-derived helium during the 1997-1998

962   seismic swarm of Umbria-Marche, Italy. Geophy. Res. Lett. 28(5), 839-842,

963   doi:10.1029/2000GL012059 (2001).

964

965   Keranen, K.M., Weingarten, M., Induced seismicity. Annu. Rev. Earth Pl. Sc. 46, 149-174.

966   doi:10.1146/annurev-earth-082517-010054 (2018).

967

968   King, C.Y., Gas geochemistry applied to earthquake prediction: An overview, Journal of Geophysical

969   Research. https://doi.org/10.1029/JB091iB12p12269 (1986).

970

971   Lai, C.G., Poggi, V., Famà, A., Zuccolo, E., Bozzoni, F., Meisina, C., Bonì, R., Martelli, L., Massa,

972   M., Mascandola, C., Petronio, L., Affatato, A., Baradello, L., Castaldini, D., Cosentini, R.M., An

973   inter-disciplinary and multi-scale approach to assess the spatial variability of ground motion for

974   seismic microzonation: the case study of Cavezzo municipality in Northern Italy, Eng. Geol. 274,

975   105722, https://doi.org/10.1016/j.enggeo.2020.105722 (2020).

976

977   Lee, H.A., Hamm, S.Y., Woo, N.C., Pilot-scale groundwater monitoring network for earthquake

978   surveillance and forecasting research in Korea. Water 13:2448, 1-19, doi:10.3390/w13172448

979   (2021).

980

981   Locati, M., Camassi, R., Rovida, A., Ercolani, E., Bernardini, F., Castelli, V., Caracciolo, C.H.,

982   Tertulliani, A., Rossi, A., Azzaro, R., D'Amico, S., Conte, S., Rocchetti, E., Antonucci, A., Database

983   Macrosismico Italiano (DBMI15), versione 4.0. Istituto Nazionale di Geofisica e Vulcanologia

984   (INGV), https://doi.org/10.13127/dbmi/dbmi15.4 (2022).

985

986   Luzi, L., Pacor, F., Ameri, G., Puglia, R., Burrato, P., Massa, M., Augliera, P., Castro, R.,

987   Franceschina, G., Lovati, S. Overview on the strong motion data recorded during the May-June 2012

988   Emilia seismic sequence. Seism. Res. Lett., 84, 4, 629-644 (2013).

989

990   Luzi, L., Puglia, R., Russo, E., D'Amico, M., Felicetta, C., Pacor, F., Lanzano, G., Çeken, U.,

991   Clinton, J., Costa, G., et al. The European strong-motion database: a platform to access accelerometric

992   data. Seismol. Res. Lett. 87, 4, doi: 10.1785/0220150278 (2016).

993

994   Malagnini, L., Pio Lucente, F., De Gori, P., Akinci, A., Munafo', I., Control of pore fluid pressure

995   diffusion on fault failure mode: Insights from the 2009 L'Aquila seismic sequence. J. Geophys. Res-

996   Sol. Ea. 117, 1-15, doi:10.1029/2011JB008911 (2012).

997

998   Mancini, S., Egidio, E., De Luca, D.A., Lasagna, M., Application and comparison of different

999   statistical methods for the analysis of groundwater levels over time: Response to rainfall and resource

1000   evolution in the Piedmont Plain (NW Italy). Science of the total Environment 846, 157479 (2022).

1001

1002   Marchetti, A. and co-Authors The Italian Seismic Bulletin: strategies, revised pickings and locations

1003   of the central Italy seismic sequence. Annals of Geophysics FAST TRACK 5/59, 10.4401/ag-7169

1004   (2016).

1005

1006   Margheriti, L. and co-Authors Seismic Surveillance and Earthquake Monitoring in Italy.

1007   Seismological Research Letters 92 (3): 1659-1671 (2021).

1008

1009   Martinelli, G., Contributions to a history of earthquake prediction research. In Pre-earthquake

1010   processes: a multidisciplinary approach to earthquake prediction studies. Editors Ouzounov, D.,

1011   Pulinets, S., Hattori, K., Taylor, P. John Wiley & Sons (2018).

1012

1013   Martinelli, G., Ciolini, R., Facca, G., Fazio, F., Gherardi, F., Heinicke, J., Pierotti, L., Tectonic-related

1014   geochemical and hydrological anomalies in Italy during the last fifty years. Minerals 11:107, 1-16,

1015   doi:10.3390/min11020107 (2021).

1016

1017   Massa M., Rizzo L.A., Ferrari E., Lovati S., Scafidi D., Puglia R., Varchetta F., D'Alema E., Mirenna

1018   S., Luzi L., MUDA geophysical and geochemical MUltiparametric DAtabase,

1019   https://doi.org/10.13127/muda (2023).

1020

1021   Massa, M., Marzorati,S., D'Alema, E., Di Giacomo, D., Augliera, P., Site Classification Assessment

1022   for Estimating Empirical Attenuation Relationships for Central-Northern Italy Earthquakes. Journal

1023   Earth. Eng. 11:6, 943-967 (2007).

1024

1025   Massa, M., Rizzo, A.L., Lorenzetti, A., Lovati, S., D'Alema, E., Puglia, R., Carannante, S., Piersanti,

1026   A., Galli, G., Cannelli, V., Luzi, L., blog INGV Terrermoti, https://ingvterremoti.com/2021/12/10/la-

1027   rete-del-lago-di-garda-una-nuova-infrastruttura-dellingv-per-il-monitoraggio-multiparametrico/   (in

1028   Italian) (2021).

1029

1030   Massa, M., Lovati, S., Puglia, R., Brunelli, G., Lorenzetti, A., Mascandola, C., Felicetta, C., Pacor,

1031   F., Luzi, L., Seismo-Stratigraphic Model for the Urban Area of Milan (Italy) by Ambient-Vibration

1032   Monitoring and Implications for Seismic Site Effects Assessment. Frontiers in Earth Science doi:

1033   10.3389/feart.2022.915083 (2022b).

1034

1035   Massa, M., Scafidi, D., Mascandola, C., Lorenzetti, A., Introducing ISMDq—A Web Portal for Real-

1036   Time Quality Monitoring of Italian Strong-Motion Data. Seismol. Res. Lett. 93 (1), 241-256,

1037   doi:10.1785/0220210178 (2022).

1038

1039   Mastrorillo, L., Saroli, M., Viaroli, F., Banzato, F., Valigi, D., Petitta, M., Sustained post-seismic

1040   effects on groundwater flow in fractured carbonate aquifers in Central Italy. Hydrological Processes

1041   https://doi.org/10.1002/hyp.13662 (2020).

1042

1043   Mazzoli, S., Santini, S., Macchiavelli, C., Ascione, A., Active tectonics of the outer northern

1044   Apennines: Adriatic vs. Po Plain seismicity and stress fields. Journal of Geodynamics 84, 62-76

1045   (2015).

1046

1047   McNamara, D.E., Buland, R.P., Ambient Noise Levels in the Continental United States. Bull. Seism.

1048   Soc. Am. 94, 4, 1517-1527, https://doi.org/10.1785/012003001 (2004).

1049

1050   Menberg, K., Blum, P., Kurylyk, B.L., Bayer, P., Observed groundwater temperature response to

1051   recent climate change. Hydrol. Earth Syst. Sci. 18, 4453-4466, doi:10.5194/hess-18-4453-2014

1052   (2014).

1053

1054   Michelini, A., Faenza, L., Lanzano, G., Lauciani, V., Jozinović D., Puglia, R., Luzi, L., The New

1055   ShakeMap in Italy: Progress and Advances in the Last 10 Yr. Seismological Research Letters 91 (1),

1056   317-333 (2020).

1057

1058   Miller, S.A., Collettini, C., Chiaraluce, L., Cocco, M., Barchi, M., Kaus, B.J.P., Aftershocks driven

1059   by a high-pressure CO_2 source at depth. Nature 427, 724-727, doi:10.1038/nature02251 (2004).

1060

1061   Ministero delle Infrastrutture e dei Trasporti Aggiornamento delle Norme Tecniche per le

1062   Costruzioni. Part 3.2.2: Categorie di sottosuolo e condizioni topografiche (in Italian), Gazzetta

1063   Ufficiale n. 42 (2018).

1064

1065   Massa M., Rizzo L.A., Ferrari E., Lovati S., Scafidi D., Puglia R., Varchetta F., D'Alema E., Mirenna

1066   S., Luzi L, MUDA: geophysical and geochemical MUltiparametric Database,

1067   https://doi.org/10.13127/muda (2023).

1068

1069   Nakamura, Y., A method for dynamic characteristics estimation of subsurface using microtremor on

1070   the ground surface. Q. Rep. Railway Tech. Res. Inst. 30 (1), 25-33 (1989).

1071

1072   Napolitano, F., De Siena, L., Gervasi, A., Guerra, I., Scarpa, R., La Rocca, M., Scattering and

1073   absorption imaging of a highly fractured fluid-filled seismogenetic volume in a region of slow

1074   deformation. Geosci. Front. 11, 989-998, doi:10.1016/j.gsf.2019.09.014 (2020).

1075

1076   Pacor, F., Paolucci, R., Ameri, G., Massa, M., Puglia R., Italian strong motion records in ITACA:

1077   Overview and record processing. Bull. Earthq. Eng. 9, 6, 1741-1759 (2011).

1078

1079   Pessina, V., Fiorini, E., A GIS procedure for fast topographic characterization of seismic recording

1080   stations. Soil Dynam. Earthq. Eng. 63, 248-258 (2014).

1081

1082   Pieri, M., Groppi, G., Subsurface Geological Structure of the Po Plain, Italy. Progetto Finalizzato

1083   Geodinamica/Sottoprogetto "Modello Strutturale" (Rome: Consiglio Nazionale delle Ricerche Publ.

1084   N° 414) (1981).

1085

1086   Pondrelli, S., Ekström, G., Morelli, A., Seismotectonic re-evaluation of the 1976 Friuli, Italy, seismic

1087   sequence. Journal of Seism., 5, 73-83 (1999).

1088

1089   Rikitake, T., Hamada, K., Earthquake prediction. In: Encyclopaedia of Physical Science and

1090   Technology, 3rd edition, Academic Press, San Diego, CA, USA 4, 743-760 (2001).

1091

1092   Rizzo, A.L., Federico, C., Inguaggiato, S., Sollami, A., Tantillo, M., Vita, F., Bellomo, S., Longo,

1093   M., Grassa, F., Liuzzo, M., The 2014 Effusive Eruption at Stromboli Volcano (Italy): Inferences From

1094   Soil CO_2 Flux and 3He/4He Ratio in Thermal Waters. Geoph. Res. Lett.

1095   http://dx.doi.org/10.1002/2014GL062955 (2015).

1096

1097   Romano, D., Sabatino, G., Magazù, S., Di Bella, M., Tripodo, A., Gattuso, A., Italiano, F.,

1098   Environmenta Earth Sciences 82, 273 (2023).

1099

1100   Russo, T.A., Lall, U., Depletion and response of deep groundwater to climate-induced pumping

1101   variability. Nature Geoscience 10, 105-108 (2017).

1102

1103   Rovida, A., Locati, M., Camassi, R., Lolli, B., Gasperini, P., The Italian Earthquake Catalogue

1104   CPTI15. Bull. Earthq. Eng. 18 (7), 2953-2984, doi:10. 1007/s10518-020-00818-y (2020).

1105

1106 Scognamiglio, L., Tinti, E., Michelini, A., Dreger, D.S., Cirella, A., Cocco, M., Salvatore, M.,

1107 Piatanesi, A., Fast Determination of Moment Tensors and Rupture History: What Has Been Learned

1108 from the 6 April 2009 L'Aquila Earthquake Sequence. Seism. Res. Lett. 81(6): 892-906 (2009).

1109

1110 Serpelloni, E., Anzidei, M., Baldi, P., Casula, G., Galvani, A., Crustal Velocity and Strain-Rate fields

1111 in Italy and Surrounding Regions: New Results From the Analysis of Permanent and Non- Permanent

1112 GPS Networks. Geophys. J. Int., 161, 3, 861-880 (2005).

1113

1114 Shinohara, H., A new technique to estimate volcanic gas composition: plume measurements with a

1115 portable multi-sensor system. J. Volcanol. Geotherm. Res. 143, 319-333 (2005).

1116

1117 Skelton, A., and co-Authors Changes in groundwater chemistry before two consecutive earthquakes

1118 in Iceland. Nature Geoscience 7, 752-756 (2014).

1119

1120 Stucchi, M., Meletti, C., Montaldo, V., Crowley, H., Calvi, G.M., Boschi, E., Seismic Hazard

1121 Assessment (2003-2009) for the Italian building code. Bull. Seism. Soc. Am. 101, 1885-1911 (2011).

1122

1123 Taylor, C.A., Stefan, H.G., Shallow groundwater temperature response to climate change and

1124 urbanization. J. Hydrol. 375, 601-612, doi:10.1016/j.jhydrol.2009.07.009 (2009).

1125

1126 Ventura, G., Di Giovambattista, R., Fluid pressure, stress field and propagation style of coalescing

1127 thrusts from the analysis of the 20 May 2012 M_L 5.9 Emilia earthquake (Northern Apennines, Italy).

1128 Terra Nova 25, 72-78, doi: 10.1111/ter.12007 (2012).

1129

1130 Weiss, A., Topographic position and landform analysis. 21st Annual Esri International User

1131 Conference, San Diego, California, 9-13 July (2001).

1132

1133 **Figure Captions**

1134

1135 **Figure 1 -** MUDA home page: https://muda.mi.ingv.it. Examples of interactive pop-ups are reported

1136 in map indicating the available main options concerning stations data and metadata, Italian seismic

1137 hazard (Stucchi et al., 2011), seismicity rate and both composite and single seismogenic sources

1138 (DISS database, DISS Working Group 2021). The base map is provided by ©OpenStreetMap

1139 contributors 2024. Distributed under the Open Data Commons Open Database License (ODbL) v1.0.

1140

1141 **Figure 2** - Target areas and relative multiparametric sites. Each panel indicates the multiparametric

1142 site (yellow triangles), the Italian seismic hazard map in terms of horizontal peak ground acceleration

1143 (PGA) with 10% probability of exceedance in 50 years on hard ground (Stucchi et al., 2011), the

1144 instrumental seismicity from 1985 (black circles, https://terremoti.ingv.it), the historical seismicity

1145 (red circles, CPTI database, Rovida et al., 2020) and the seismogenic sources (CSS-DISS database,

1146 DISS Working Group 2021). The base maps are provided by ©OpenStreetMap contributors 2024.

1147 Distributed under the Open Data Commons Open Database License (ODbL) v1.0.

1148

1149 **Figure 3** - Dynamic multiparametric data web page: https://muda.mi.ingv.it/dat.php. From top to

1150 bottom: hydrogeochemical data (light blue panels: water level, m; water electrical conductivity,

1151 µS/cm; water temperature, °C), meteorological data (green panel: soil temperature, °C; rain, mm),

1152 seismic data (light brown panels: RMS, ground motion velocity, cm/s; FFT, cm/s/Hz; FFT(f),

1153 cm/s/Hz), CO_2 data (grey panels: soil flux, $g*m^{-2}*d^{-1}$; humidity, %; soil temperature, °C), Radon data

1154 on air (yellow panel: Bq/m^3). All time series (*csv* format) and each single graph (*pdf*, *png* formats)

1155 are downloadable by using the menu available in the top right corner of each panel.

1156

1157 **Figure 4** - Multiparametric site web page: https://muda.mi.ingv.it/stazione.php. The single site web

1158 page indicates the main features of both instrumentation and installation, downloadable thematic

1159 maps such as the geological map (1:100.000, Società Geologica Italiana

1160 http://www.isprambiente.gov.it/it/cartografia/), the topographic map (base at 1:25.000, Istituto

1161 Geografico Militare, http://www.igmi.org/prodotti/cartografia/carte_topografiche/), log and

1162 stratigraphy concerning the available wells for water, a preliminary geophysical soil characterization

1163 in term of horizontal to vertical spectral ratio performed on ambient seismic noise and the complete

1164 time hydrogeochemical time series. Sources for base maps: Esri, DigitalGlobe, GeoEye, i-cubed,

1165 USDA FSA, USGS, AEX, Getmapping, Aerogrid, IGN, IGP, swisstopo, and the GIS User

1166 Community.

1167

1168 **Figure 5 -** MUDA data base scheme and processing flow chart.

1169

1170 **Figure 6** - Single station data set for multiparametric sites having at least 6 months of data and three

1171 different types of acquisition. S: seismic data (red); Id: hydrogeochemical data (blue); M:

1172 meteorological data (green); R: Radon data (grey); C: CO_2 data (yellow). Yellow and orange stars

1173 indicate recorded earthquakes at each site with magnitude (Moment or Local) lower and higher then

1174 4, respectively.

1175

1176 **Figure 7** - Quality check of seismic data at Oppeano site (table 1).

1177 Panel *a* (top): timeseries recorded on December, 29, 2020, by IV.OPPE station

1178 (https://terremoti.ingv.it/instruments/station/OPPE) showing consecutive earthquakes: the first, with

1179 M_w=6.3, occurred in Croatia land (https://terremoti.ingv.it/event/25870121) 450 km East of IV.OPPE

1180 and the others with epicentres 11 km South-West of IV.OPPE with maximum M_w=3.9

1181 (https://terremoti.ingv.it/event/25871441). Earthquakes origin times (UTC) are reported in the top

1182 panel *a*).

The bottom panel *a*) shows the FFT functions calculated considering 15 frequency intervals from 0.1 to 20 Hz, considering 288 consecutive 5 minutes-time windows (i.e. 24 hours) selected on the vertical component of motion.

Panel *b*: from top to bottom, the RMS, the ground motion velocity and the mean FFT calculated for 288 consecutive time windows with duration of 5 minutes. Red, blue and green indicate the vertical, the North-South and the East-West horizontal components of motion. The black solid lines indicate the cumulative functions.

Figure 8 - Example of multiparametric data recorded at Bondo site (table 1). Panel *a* shows the hydrogeochemical data recorded in the time period from October 15 to November 15, 2023: black, red and green solid lines indicate the water level (m), the electrical conductivity (μS/cm) and the water temperature (°C) variations, respectively.

The panel *b* shows the seismic data recorded at ZO.PDN3 station (table 2) on October, 31 and November, 1, 2023, while the panel *c* shows the polarization analysis in terms of rotated horizontal to vertical spectral ratio.

Figure 9 - Radon time series (Bq/m^3, black lines) recorded at Bondo (panel *a*) and Montelungo (panel *b*) multiparametric sites. Soil temperature (°C, green lines) and rain (mm, light blue lines) are also indicated. At the top of each panel seasons are indicated (Aut=Autumn, Win=Winter, Spr=Spring, Sum=Summer).

Figure 10 - Panel *a*: CO$_2$ flux (g*m^{-2}*d^{-1}, black line) recorded at NIRANO multiparametric site. Red and green solid lines indicate the smoothing function of CO$_2$ flux and the temperature (°C), respectively. The orange box indicates the time window represented in the bottom panel.

Panel *b*: detailed monitoring for period October 25 to November 15, 2023, where a seismic sequence, with maximum local magnitude of 3.5 (vertical yellow dashed lines) occurred in correspondence of

1209   the Nirano's Mud-Volcanoes. Dotted and dashed orange lines indicate the mean values +/- 1-standard

1210   deviation of CO_2 flux recorded during the analysed time period. Rain values (mm, light blue) and soil

1211   temperature (°C) are also indicated. Black dots indicate the CO_2 measures ($g*m^{-2}*d^{-1}$).

1212

1213   **Figure 11** - Groundwater recharge at Volargne (panel *a*) and Fonte (panel *b*) sites (table 1) recorded

1214   on October 30, 2023. In both panels, black, red and green solid lines indicate the water level (m), the

1215   electrical conductivity (µS/cm) and the water temperature (°C) variations, respectively, while the blue

1216   solid lines indicate the cumulative rain.

1217

1218   **Table captions**

1219

1220   **Table 1** - Monitoring multiparametric sites at present include in MUDA.

1221

1222   **Table 2** - Main features of hydrogeochemical probes and seismic monitoring stations. Grey cells

1223   indicate well with thermalism (i.e. Triponzo site), while the black cells indicate the borehole seismic

1224   sensor installed 150 m depth at Oppeano site.

1225   In detail,

1226   water level: water depth below ground level at the time of installation;

1227   water column: water column above the sensor at the time of installation;

1228   water temperature: average values of water temperature and specific electrical conductivity. It is

1229   worth noting that for some sites the averages are merely indicative as they refer to short recording

1230   intervals (see Table 1 for installation dates). Specific electrical conductivity is recalculated at 25 °C.

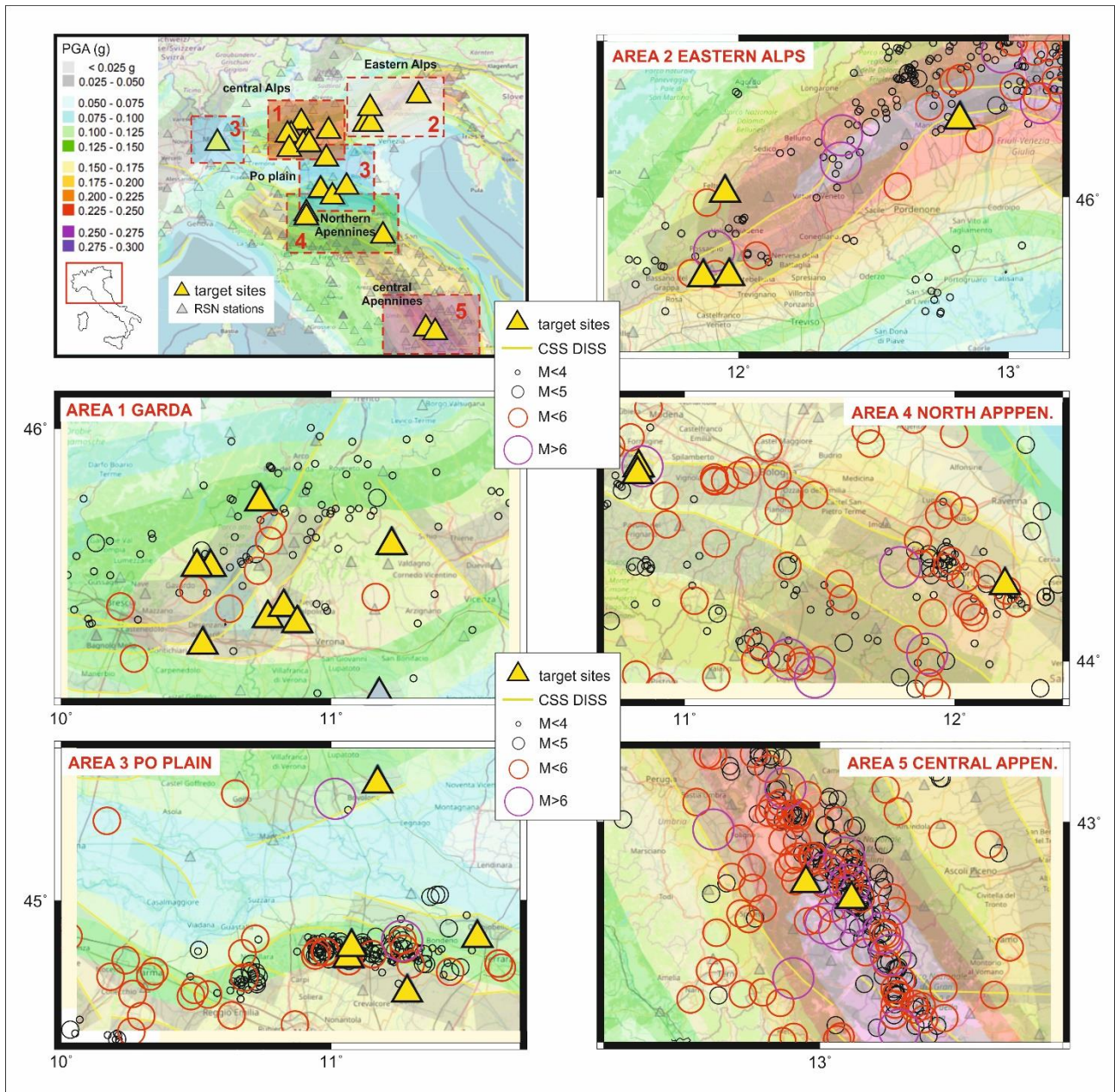1231   water pump: absence (0) or presence (1) of water pump.

1232

1233
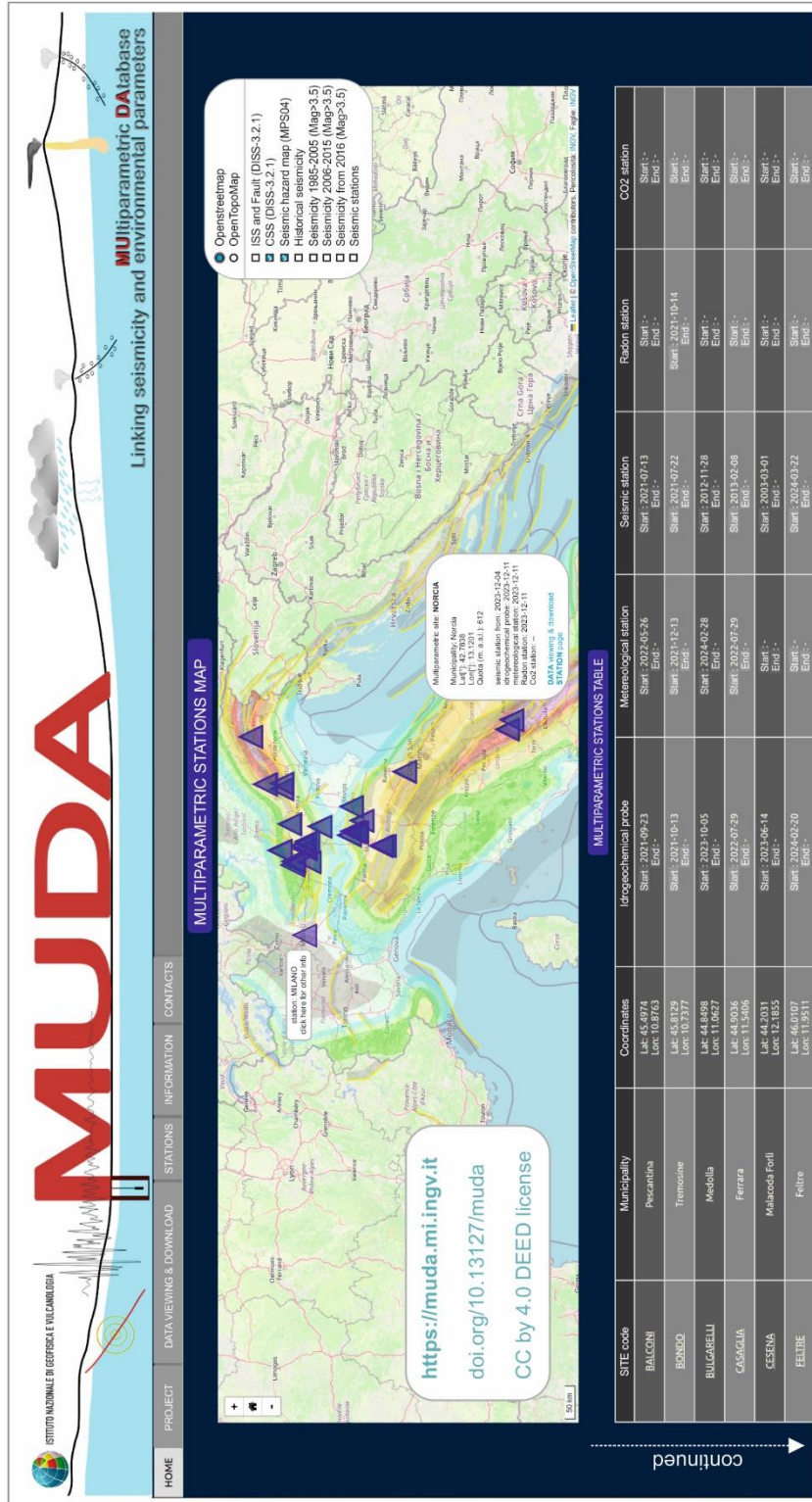
1234

1235   Figure 1

1236

49

1237

1238

1239 Figure 2
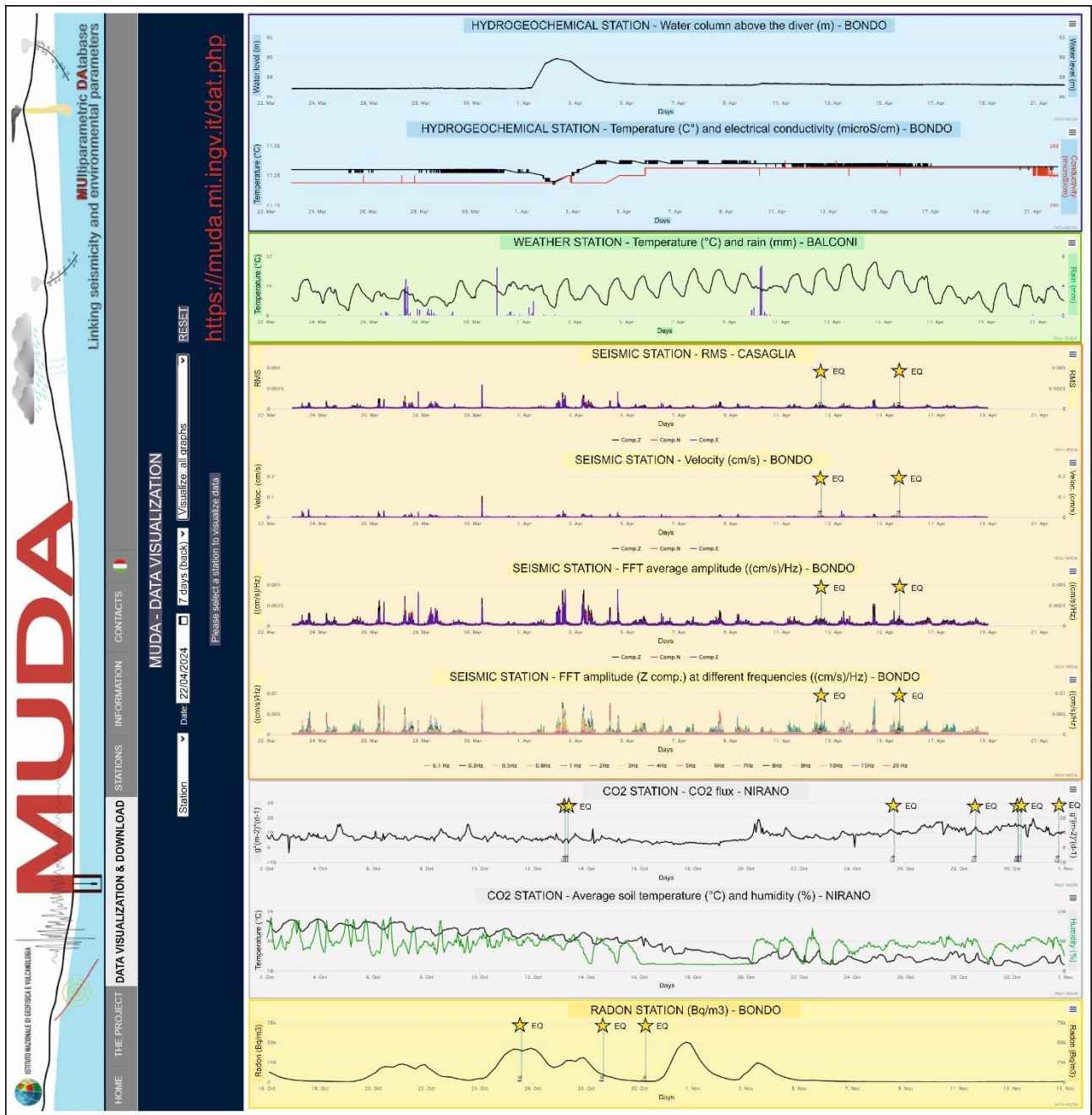
1240

1241

1242

1243

1244

1245

1246

1247

1248

1249 Figure 3

1250

1251

1252

1253
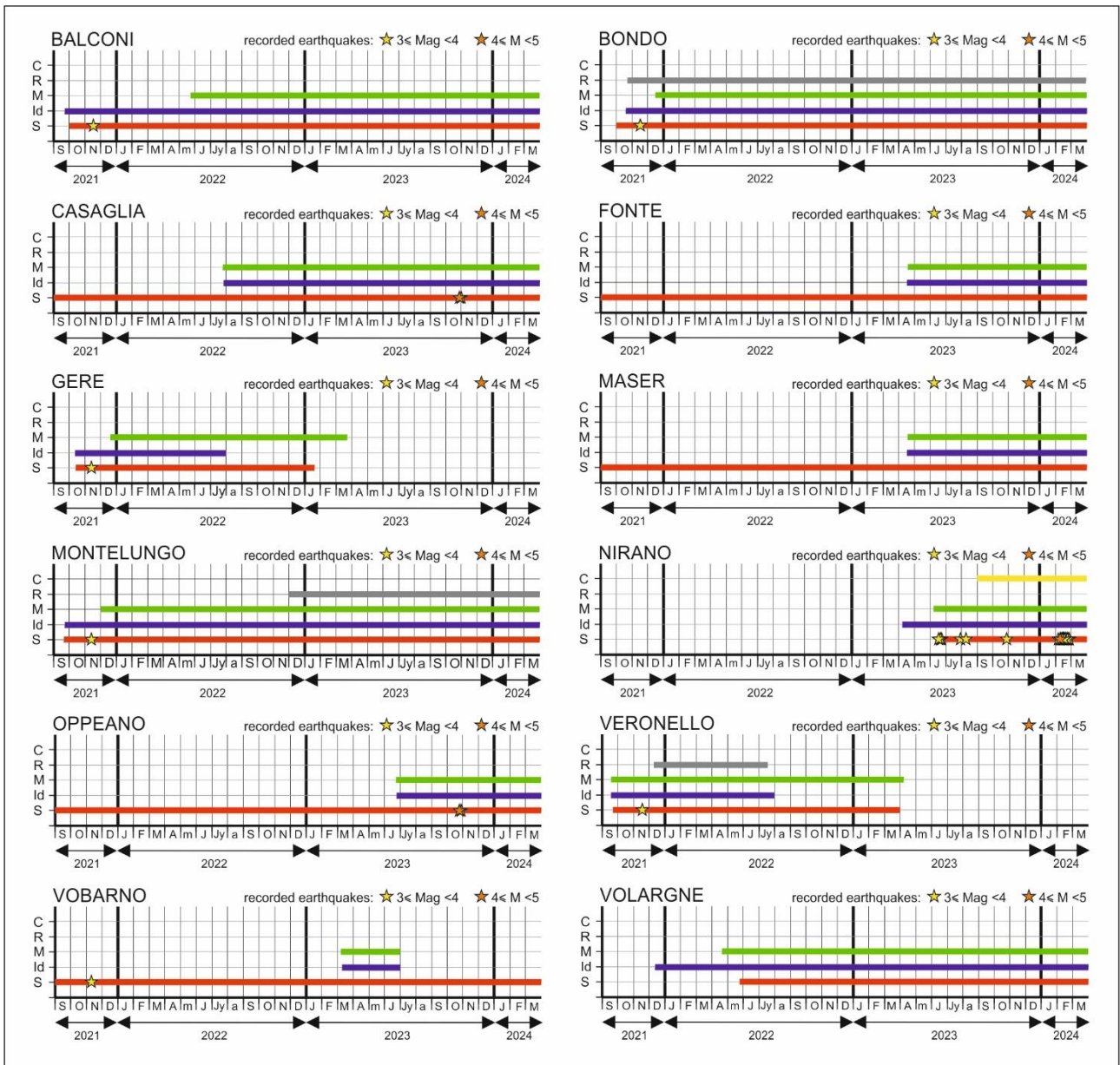
1254

1255
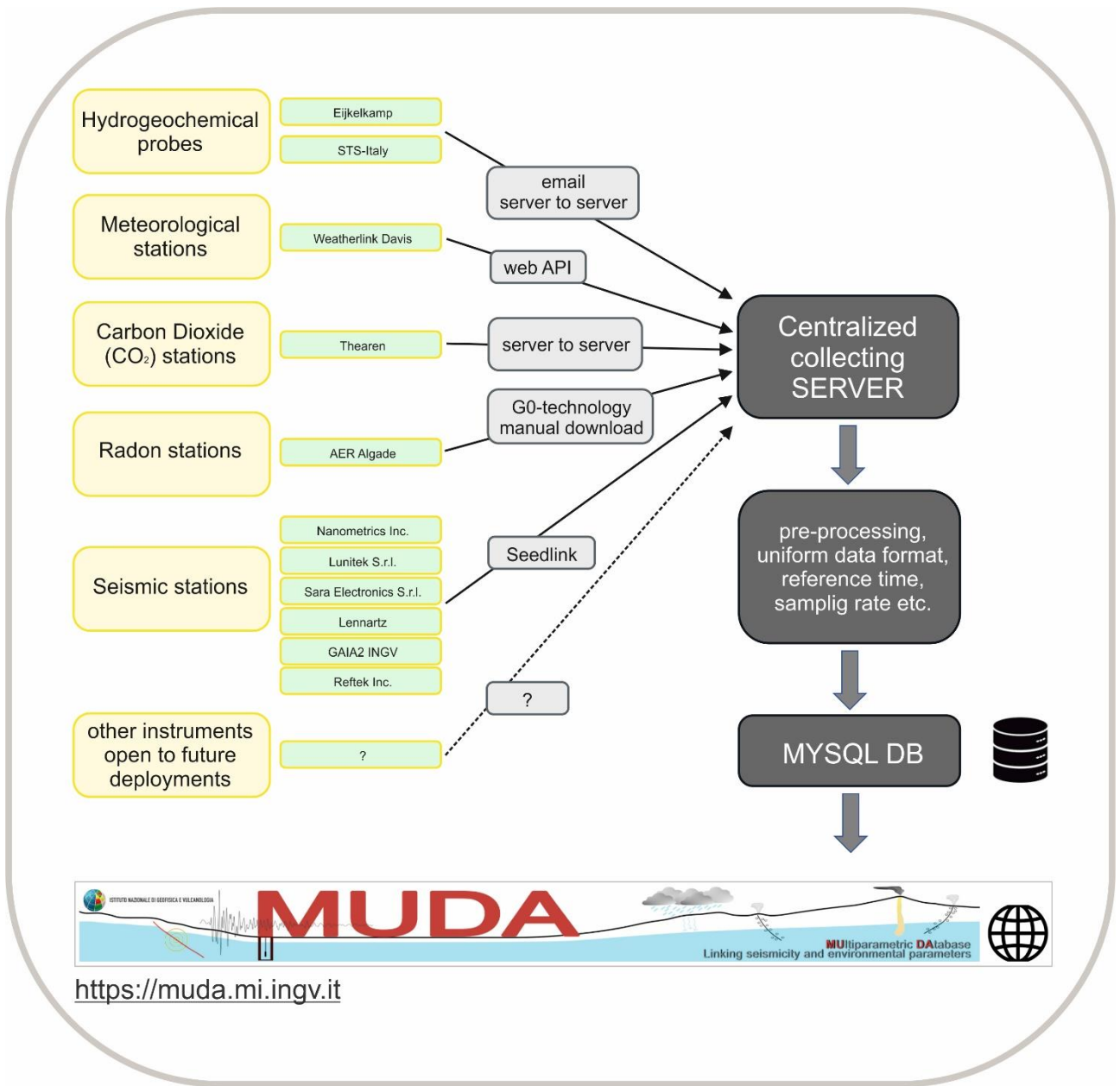
Figure 4

1261

1262

1263   Figure 5

1264

1265
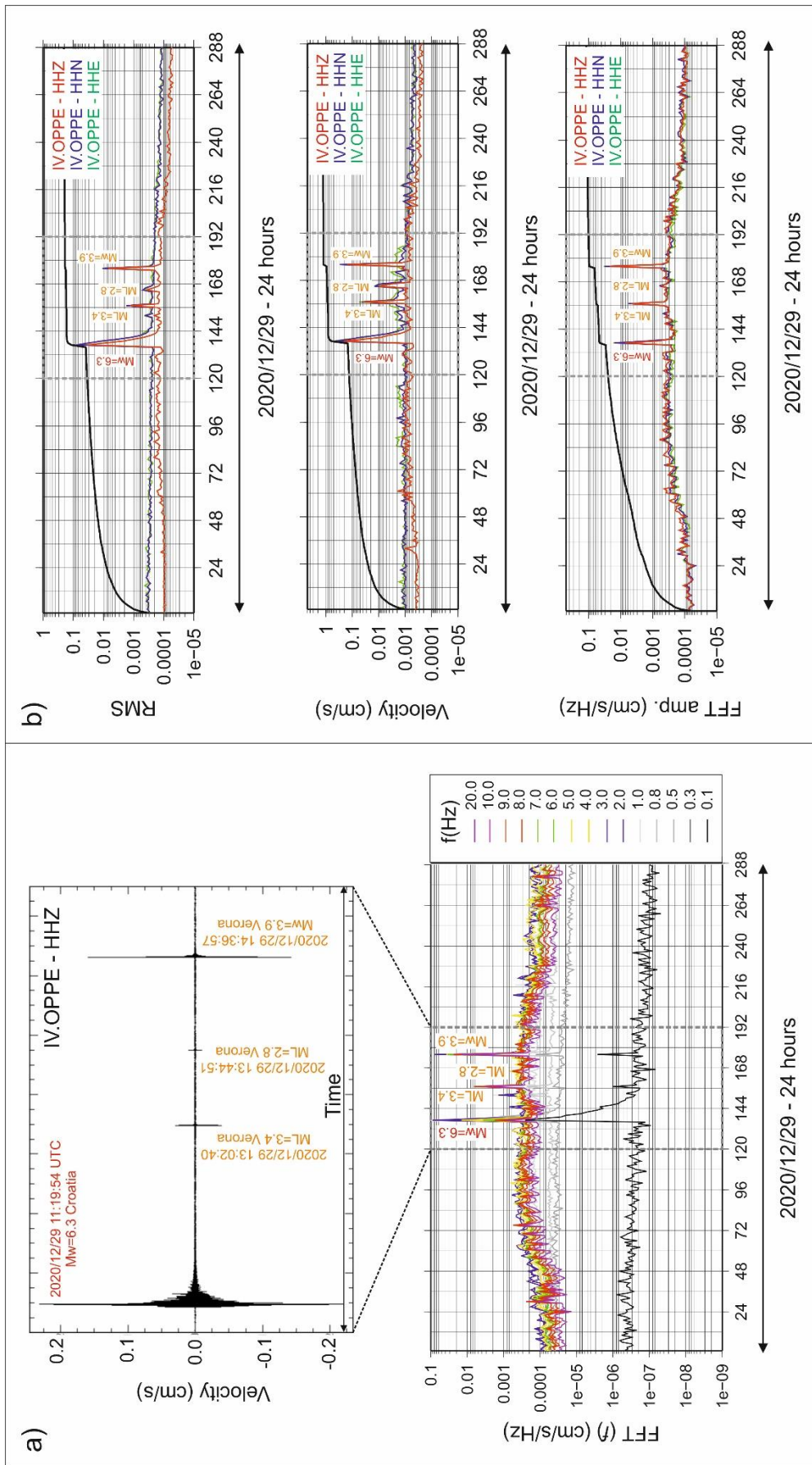
1266

1267

1268

1269

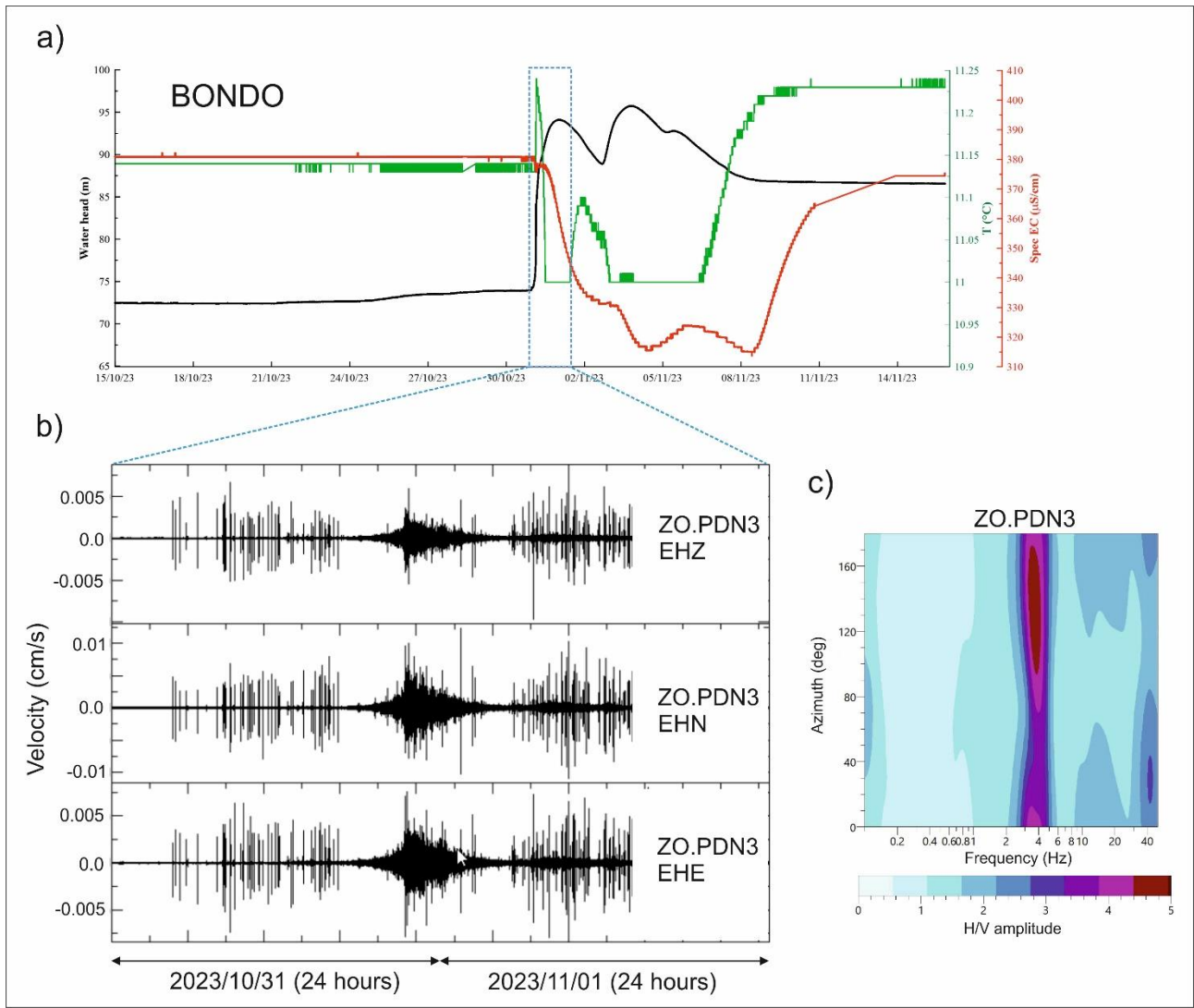1270

1271

1272

1273   Figure 6

1281

1282

1283   Figure 7

1284

1285

1286   Figure 8

1287

1288

1289

1290

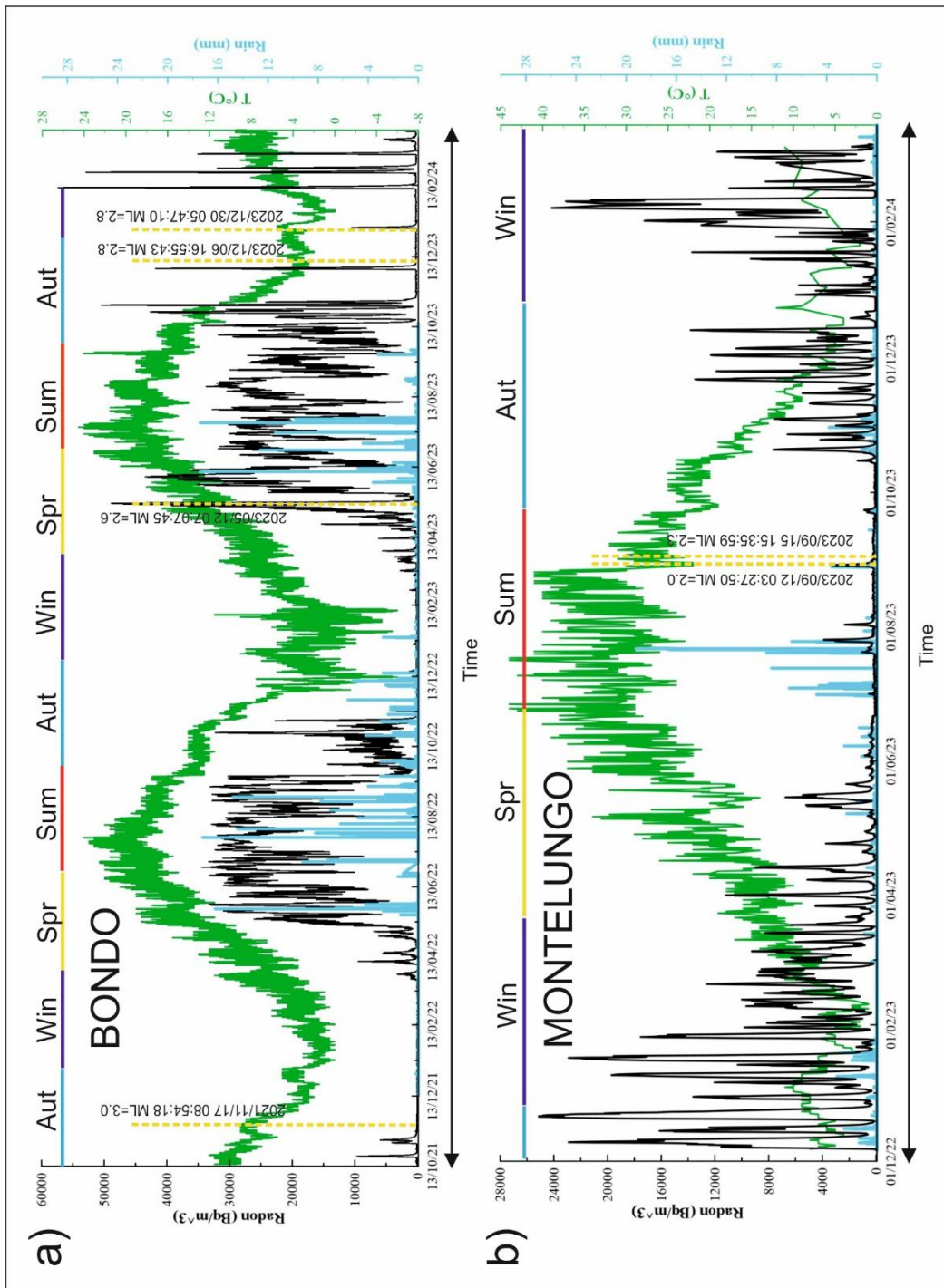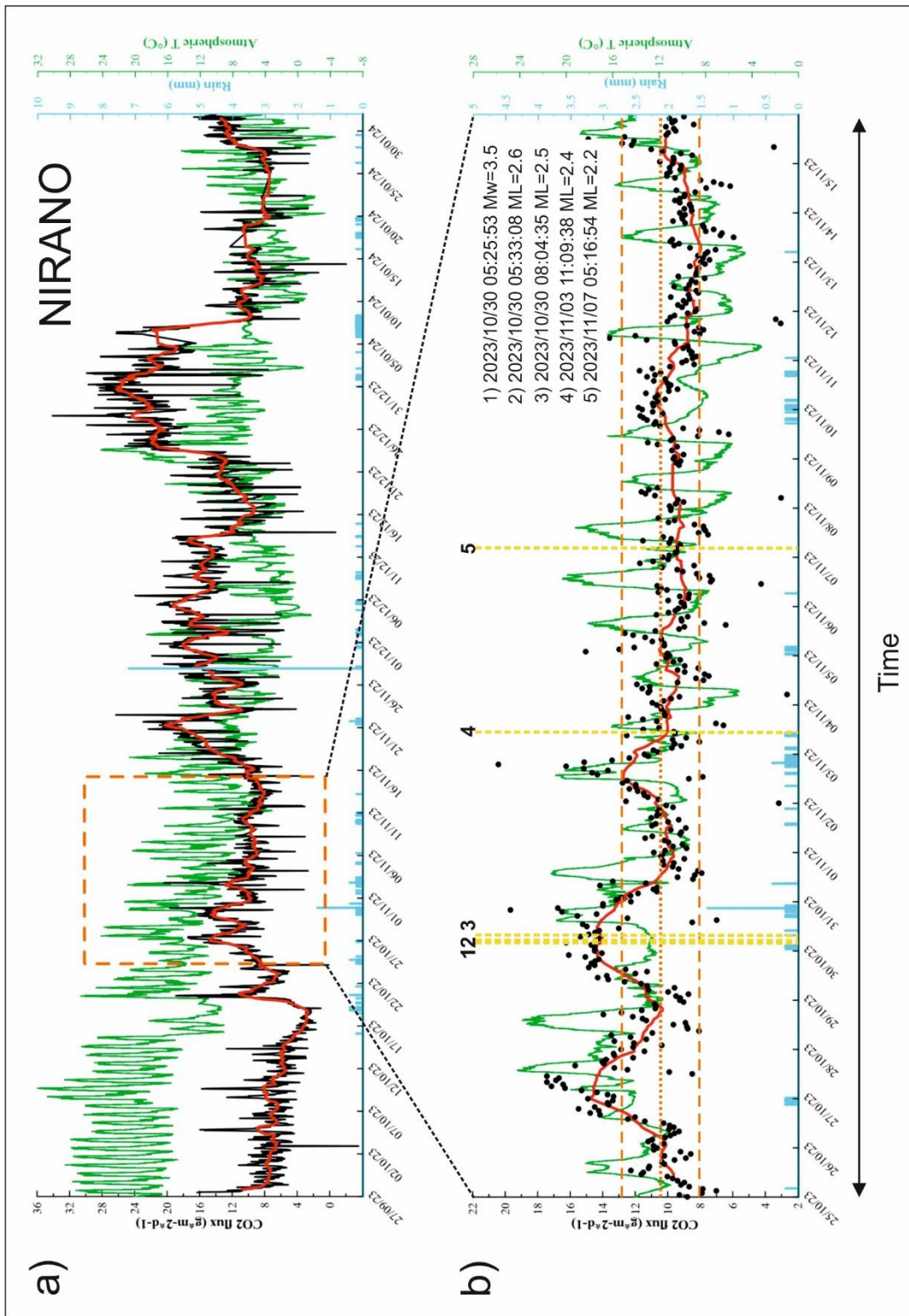1291

1292

1293

1294

1295

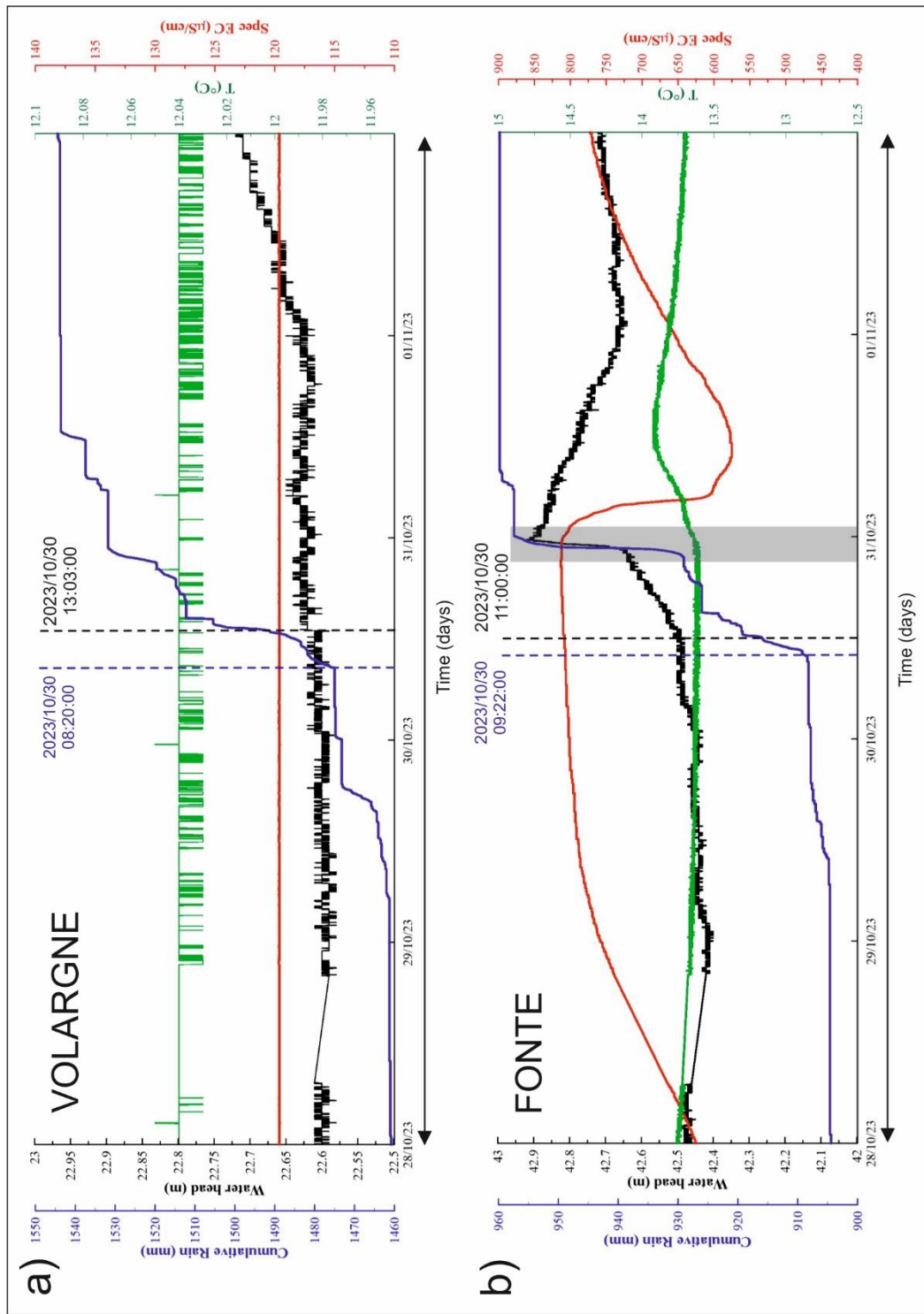1296

1297

1298 Figure 9

1299

1300

1301

1302

1303

1304

1305

1306   Figure 10

1307

1308

1309

1310

1311

1312   Figure 11

1313

1314

1315

59

Table 1

CODE	Municipality	AREA	LAT [°]	LON [°]	idro-geochemical	weather	seismic	Radon	CO2
BALCONI	Pescantina	1	45.4974	10.8763	start 2021-09-23	start 2022-05-26	start 2021-07-13	/	/
BONDO	Tremosine	1	45.8129	10.7377	start 2021-10-13	start 2021-12-13	start 2021-07-22	start 2021-10-14	/
BULGARELLI	Medolla	3	44.8498	11.0627	start 2024-02-28	start 2024-02-28	start 2012-11-28	/	/
CASAGLIA	Ferrara	3	44.9036	11.5406	start 2022-07-29	start 2022-07-29	start 2013-02-08	/	/
CESENA	Malacoda Forlì	4	44.2031	12.1855	start 2024-02-20	/	start 2003-03-01	/	/
FELTRE	Feltre	2	46.0107	11.9511	start 2024-02-20	/	/	/	/
FONTE	Fonte	2	45.7949	11.8697	start 2023-04-18	start 2023-04-17	start 2011-11-17	/	/
GERE	Gardone Riviera	1	45.6422	10.5484	start 2021-10-12 - end 2022-07-30	start 2021-12-02 - end 2023-03-25	start 2021-10-12 - 2023-01-18	/	/
MASER	Maser	2	45.7969	11.9658	start 2023-04-17	start 2023-04-17	start 2011-11-17	/	/
MEDOLLA	Medolla	3	44.8492	11.0734	start 2024-02-20	start 2024-02-28	start 2012-11-28	/	/
MILANO	Milano	3	45.4972	9.1812	start 2024-03-12	start 2024-03-12	start 2012-01-27	/	/
MIRANDOLA	Mirandola	3	44.8812	11.0782	start 2024-02-23	start 2024-02-23	start 2012-11-28	/	/
MONTELUNGO	Desenzano del Garda	1	45.4429	10.5256	start 2021-09-14	start 2021-11-30	start 2021-07-30	start 2022-12-06	/
NIRANO	Fiorano Modenese	4	44.5141	10.8255	start 2023-04-04	start 2023-06-06	start 2023-06-23	/	start 2023-09-27
NIRANO1	Fiorano Modenese	4	44.5002	10.8163	start 2024-02-20	start 2024-02-20	start 2023-06-23	/	/
NORCIA	Norcia	5	42.7838	13.1201	start 2023-12-11	start 2023-12-11	start 2023-12-04	start 2023-12-11	/
OPPEANO	Oppeano	3	45.3082	11.1723	start 2023-06-29	start 2023-06-21	start 2023-02-16	/	/
RECOARO	Recoaro Terme	1	45.6998	11.2217	start 2024-01-30	start 2024-01-30	/	/	/
RECOARO1	Recoaro Terme	1	45.7005	11.2215	start 2024-01-30	start 2024-01-30	/	/	/
RENAZZO	Renazzo	3	44.7624	11.2836	start 2024-02-20	/	start 2003-10-11	/	/
SECCHIA	Concordia Secchia	3	44.9245	11.0183	start 2024-03-14	start 2024-03-20	start 2012-11-28	/	/
TOPPO	Toppo di Travesio	2	46.1985	12.8171	start 2024-02-25	/	/	/	/
TRIPONZO	Triponzo	5	42.8400	12.9480	start 2023-12-12	start 2023-12-12	start 2023-12-04	start 2023-12-12	/
VERONELLO	Bardolino	1	45.5098	10.7645	start 2021-09-14 - end 2022-08-01	start 2021-10-19 - end 2023-04-07	start 2021-07-08 - end 2023-04-07	start 2021-12-17 - end 2022-07-08	/
VOBARNO	Vobarno	1	45.6428	10.5035	start 2023-03-10 - end 2023-06-21	start 2023-03-10 - end 2023-06-21	start 2021-07-08	/	/
VOLARGNE	Dolcè	1	45.5397	10.8235	start 2021-12-16	start 2022-05-20	start 2022-04-12	/	/

Table 2

CODE	AREA	Geology (100k)	Topography	SITE TYPE	WELL DEPTH (m)	WATER LEVEL (m)	WATER COLUMN (m)	WATER TEMPERATURE[c] (°C)	WATER SPECIFIC EC[c] (µS/cm)	WATER PUMP	SEISMIC NET	SEISMIC CODE	RECORDER	SENSOR
BALCONI	1	fluvio-glacial deposits	plain	well	100	53.3	46.7	14.1	873	1	ZO	PDN2	Lunitek ATLAS	TELLUS-5s
BONDO	1	alluvial deposits	valley	well	180	44	136	11.1	377	0	ZO	PDN3	Reftek-130	LENNARTZ-5s
BULGARELLI	3	alluvial deposits	plain	well	8	1.5	6.5	14.5	2639	1	IV	CAVE	GAIA2	TRILLIUM-120s
CASAGLIA	3	alluvial deposits	plain	well	130	3.5	126.5	17.2	3616	0	IV	FERS	GAIA2	TELLUS-5s
CESENA	4	alluvial deposits	plain	well	8.3	3.1	5.2	16.0	1338	0	IV	BRSN	GAIA2	LENNARTZ-1s
FELTRE	2	limestone	relief	spring	/	/	/	13.4	488	0	/	/	/	/
FONTE	2	sandstone	relief	well	120	7.7	112.3	13.5	840	0	IV	ASOL	Lunitek ATLAS	TELLUS-5s
GERE	1	fluvio-glacial deposits	valley	well	60	31.3	28.7	10.3	406	1	ZO	PDN6	Lunitek ATLAS	TELLUS-5s
MASER	2	sandstone	relief	well	157	71.3	85.7	13.2	511	0	IV	ASOL	Lunitek ATLAS	TELLUS-5s
MEDOLLA	3	alluvial deposits	plain	well	50	3	47	15.3	5190	0	IV	CAVE	GAIA2	TRILLIUM-120s
MILANO	3	alluvial deposits	plain	well	152	18	135	14.0	250	0	IV	MILN	GAIA2	TRILLIUM-40s
MIRANDOLA	3	alluvial deposits	plain	well	300	5.4	294.6	17.2	87864	1	IV	CAVE	GAIA2	TRILLIUM-120s
MONTELUNGO	1	morainic deposits	hill	well	150	52.8	97.2	15.3	885	0	ZO	PDN4	Reftek-130	LENNARTZ-5s
NIRANO	4	mudstone	hill	mudhole	11	0	11	16.2	12024	0	ZO	PDN10	GAIA2	LENNARTZ-5s
NIRANO1	4	mudstone	hill	mudhole	11	0	11	14.8	2873	0	ZO	PDN10	GAIA2	LENNARTZ-5s
NORCIA	5	alluvial deposits	valley	well	64	30	34	12.0	535	1	ZO	PDN11	Reftek-130	LENNARTZ-5s
OPPEANO	3	alluvial deposits	plain	well	60	4.6	55.4	13.9	607	0	ZO	PDN9	SARA-SL06	SARA-SS08-120s
RECOARO	1	sandstone	relief	spring	/	/	/	11.4	2148	0	ZO	PDN13	Lunitek ATLAS	TELLUS-5s
RECOARO1	1	sandstone	relief	spring	/	/	/	11.3	3724	0	ZO	PDN13	Lunitek ATLAS	TELLUS-5s
RENAZZO	3	alluvial deposits	plain	well	6	1.5	4.5	17.4	1193	0	IV	RAVA	GAIA2	LENNARTZ-5s
SECCHIA	3	alluvial deposits	plain	mudhole	1	0	1	17.5	2343	0	IV	CAVE	GAIA2	TRILLIUM-120s
TOPPO	2	alluvial deposits	valley	well	300	114	186	12.7	591	0	/	/	/	/
TRIPONZO	5	limestone	crest	well	53	3.1	49.9	29.7	2487	1	ZO	PDN12	Reftek-130	LENNARTZ-5s
VERONELLO	1	fluvio-glacial deposits	hill	well	198	90	108	14.0	703	0	ZO	PDN1	Lunitek ATLAS	TELLUS-5s
VOBARNO	1	alluvial deposits	valley	well	36	11.2	24.8	13.3	240	0	IV	VOBA	Lunitek ATLAS	TELLUS-5s
VOLARGNE	1	fluvio-glacial deposits	valley	well	99	50	49	12.0	129	0	ZO	PDN8	Reftek-130	LENNARTZ-5s